Chapter 9

Global Ocean Carbon Cycle Modeling

Scott C. Doney · Keith Lindsay · J. Keith Moore

9.1 Introduction

One of the central objectives of the Joint Global Ocean Flux Study (JGOFS) is to use data from the extensive field effort to improve and evaluate numerical ocean carbon cycle models. Substantial improvements are required in the current suite of numerical models if we are to understand better the present ocean biogeochemical state, hindcast historical and paleoclimate variability, and predict potential future responses to anthropogenic perturbations. Significant progress has been made in this regard, and even greater strides are expected over the next decade as the synthesis of the JGOFS data sets are completed and disseminated to the scientific community. The goals of this chapter are to outline the role of modeling in ocean carbon cycle research, review the status of basin to global-scale modeling, and highlight major problems, challenges, and future directions.

Marine biogeochemical models are quite diverse, covering a wide range of complexities and applications from simple box models to global 4-D (space and time) coupled physical-biogeochemical simulations, and from strict research tools to climate change projections with direct societal implications. Model development and usage are strongly shaped by the motivating scientific or policy problems as well as the dynamics and time/space scales considered. A common theme, however, is that models allow us to ask questions about the ocean we could not address using data alone. In particular, models help researchers quantify the interactions among multiple processes, synthesize diverse observations, test hypotheses, extrapolate across time and space scales, and predict future behavior.

A well posed model encapsulates our understanding of the ocean in a mathematically consistent form. Many, though not all, models can be cast in general form as a coupled set of time-dependent advection, diffusion, reaction equations:

$$\frac{\partial X}{\partial t} + \vec{u}\nabla X - \nabla(K\nabla X) = \text{sources/sinks} \qquad (9.1)$$

where X refers to a set of prognostic or predicted variables (e.g., temperature, phytoplankton biomass, dissolved inorganic carbon). The second and third terms on the left hand side of the equation describe the physical processes of advection and mixing, respectively. All of the chemical and biological interactions are subsumed into the final source/sink term(s) on the right hand side, which often involve complex interactions among a number of prognostic variables. In addition, the model may require external boundary conditions (e.g., solar radiation, wind stress, dust deposition) and, for time varying problems, initial conditions. The model equations are then solved numerically by integrating forward in time for X.

Numerical models cannot capture all of the complexity of the real world. Part of the art of modeling is to abstract the essence of a particular problem, balancing model complexity with insight. Many processes must be either parameterized in a simple fashion or neglected altogether. For example, the biophysical details of photosynthesis, though quite well known, may not necessarily be crucial and certainly not sufficient for simulating the seasonal bloom in the North Atlantic. On the other hand, a number of key processes (e.g., phytoplankton mortality, the controls on community structure) are not well characterized and are often used as model tuning parameters.

As opposed to much of ocean physics, fundamental relationships either are not known or may not exist at all for much of marine biogeochemistry. Therefore, ocean biogeochemical modeling is inherently data driven. The JGOFS field data are invaluable in this regard, providing the basis for highlighting model deficiencies, developing improved parameterizations, and evaluating overall model performance. The desire for increasing model realism and sophistication must be tempered by the realization that models can quickly outstrip the ability to parameterize the appropriate processes or evaluate the overall simulation. Inverse methods and data assimilation will certainly help in this regard, but the true benefits will only be gained when the underlying models rest on a sound, mechanistic basis.

Broadly speaking, much of current ocean carbon cycle modeling can be condensed into a few overarching scientific questions that match well with the other individual chapters of this book. These include: What are

the physical and biological controls on primary, new and export production? What are the roles of multiple limiting nutrients, mesoscale variability and trophic structure? How are organic and inorganic carbon transported, transformed and remineralized below the surface layer? How much anthropogenic carbon does the ocean take up and where? How does ocean biogeochemistry respond to climate variability and are there feedbacks on climate change? Ocean carbon modeling is a diverse and growing field and can not be covered comprehensively in a single chapter. Rather, we present an overview of the current state and major issues involving ocean biogeochemical and ecosystem modeling drawing mostly on specific examples from the NCAR modeling program.

Historically, global ocean biological and chemical modeling has evolved along three related, though often distinct, paths. First, a number of early efforts were directed toward improving oceanic anthropogenic carbon uptake estimates, building on simple box models and coarse resolution ocean physical general circulation models (GCMs). Transient tracer simulations (radiocarbon, tritium, chlorofluorocarbons) developed in conjunction as a way to assess model physical circulation and mixing. Second, biogeochemical carbon cycle models, while often relying on the same physical model frameworks, were developed to improve our understanding of the dynamics controlling large-scale biogeochemical fields (e.g., surface pCO_2, subsurface nutrient, oxygen and dissolved inorganic carbon distributions) and their responses to climate variability and secular change (e.g., glacial-interglacial transition and greenhouse warming). The treatment of biological processes in this class of models has been rather rudimentary in most cases. Third, marine ecosystem models have been focused much more on the details of biological interactions within the upper ocean, tracking the controls on upper ocean primary and export production as well as the flow of mass and energy though the marine food web. These models often are created for specific biogeographical regions commonly based on local surface or 1-D time-series data sets. More recently, ecosystem models have been extended to basin and global scale. One of the most important trends in the field is the unification of these three approaches, leading ultimately to a coherent modeling framework linking ocean physics, biology and chemistry over a range of time and space scales.

9.2 Anthropogenic Carbon Uptake, Transient Tracers, and Physics

An initial and ongoing focus of ocean biogeochemical modeling research is to quantify the rate at which the ocean takes up transient tracers and excess anthropogenic CO_2. The water column and upper few meters of marine sediments contain the largest mobile, natural reservoir of carbon on time-scales of 10^2 to 10^5 years. With about 50 times more carbon than that stored in the atmosphere (Fig. 9.1) (Sarmiento and Sundquist

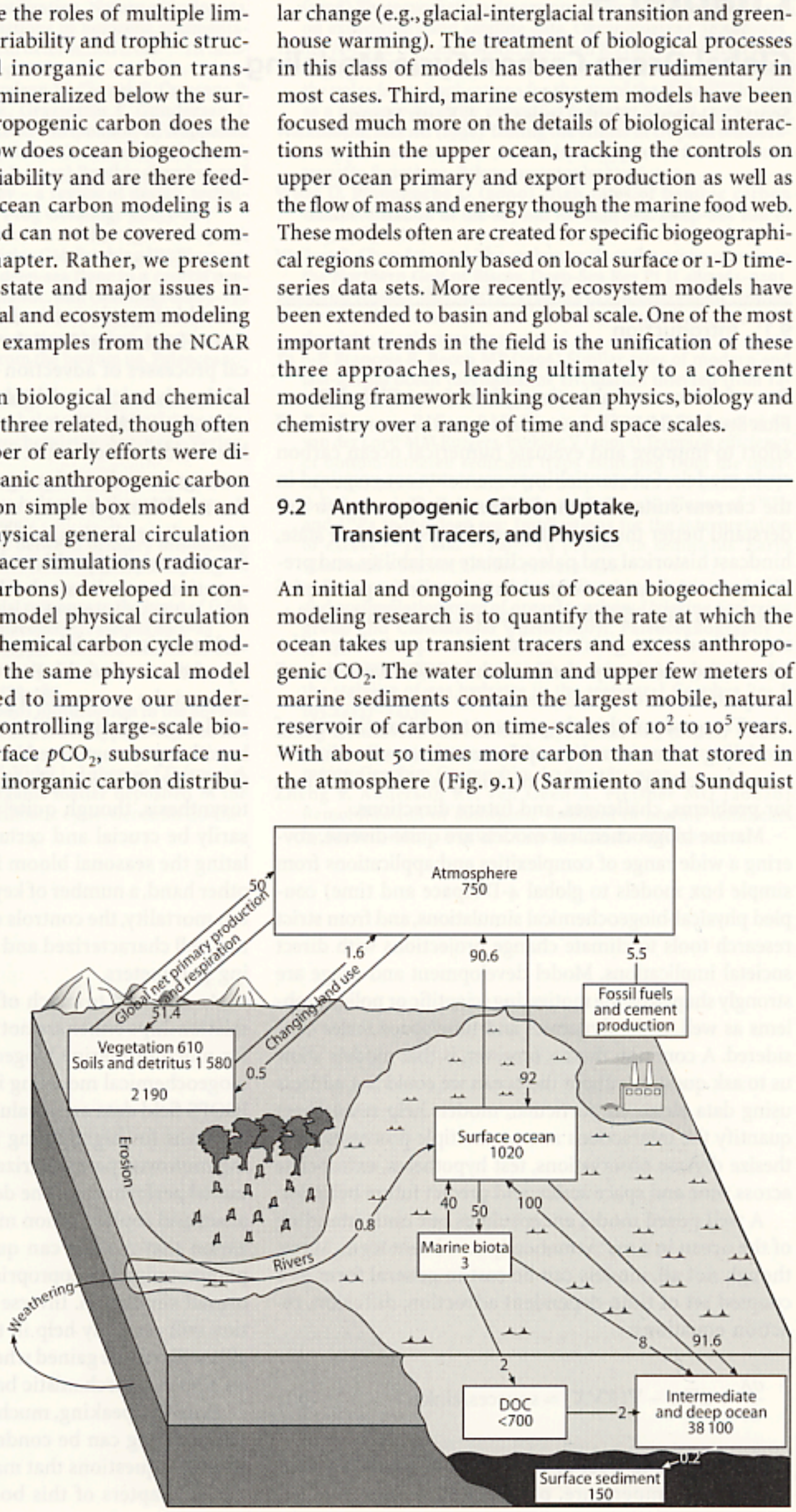

Fig. 9.1. Schematic of present global carbon cycle budget. The budget includes the natural background cycle as well as anthropogenic perturbations. Reservoir sizes are given in units of Pg C (1 Pg equals 10^{15} g), while fluxes are given in Pg C yr^{-1} (adapted from Schimel et al. (1995) and US CCSP (1999))

1992; Siegenthaler and Sarmiento 1993), the ocean will serve as the ultimate sink for about 90% of human fossil fuel emissions (Archer et al. 1998). Anthropogenic carbon uptake is often computed as a passive perturbation to the natural dissolved inorganic carbon (DIC) field (Sarmiento et al. 1992), a fairly reasonable assumption for the pre-industrial to the present time period. Under these conditions (i.e., fixed circulation and background biogeochemical cycles), net carbon uptake is simply a matter of ocean physics, primarily determined by the ventilation time-scales exposing deep water to the surface and, to a much lesser degree, air-sea gas exchange. The invasion into the ocean of transient tracers such as radiocarbon, tritium, and the chlorofluorocarbons provides a direct, often quite dramatic illustration of ocean ventilation and is commonly used either to calibrate/evaluate ocean physical models or as proxies for anthropogenic CO_2 uptake.

Early attempts to calculate ocean CO_2 uptake in the 1970s and 1980s relied heavily on ocean box and 1-D advection diffusion models of varying complexity (Oeschger et al. 1975; Siegenthaler and Oeschger 1978; Siegenthaler and Joos 1992). This class of models represents, in a fairly crude, schematic form, the basics of ocean thermocline ventilation and thermohaline circulation. The crucial model advection and mixing parameters are typically set by calibrating simulated transient tracer distributions (tritium, natural and bomb radiocarbon) to observations. More recently, such models have mostly been supplanted by full 3-D general circulation models for the anthropogenic CO_2 question. But because they are simple to construct (and interpret) and computationally inexpensive, box models and a related derivative the 2-D, zonally averaged basin model (Stocker et al. 1994) continue to be used today for a number of applications requiring long temporal integrations including paleoceanography (Toggweiler 1999; Stephens and Keeling 2000) and climate change (Joos et al. 1999). Some caution is advised, however, as recent studies (Broecker et al. 1999; Archer et al. 2000) clearly demonstrate that box model predictions for key carbon cycle attributes can differ considerably from the corresponding GCM results.

Ocean general circulation model studies of anthropogenic carbon uptake date back to the work of Maier-Reimer and Hasselmann (1987) and Sarmiento et al. (1992), and the number of model estimates (and modeling groups) for CO_2 uptake has increased significantly over the 1990s. For example, more than a dozen international groups are participating in the IGBP/GAIM Ocean Carbon Model Intercomparison Project (OCMIP; *http://www.ipsl.jussieu.fr/OCMIP/*). These numerical experiments are closely tied to and greatly benefit from efforts to evaluate ocean GCMs using hydrographic (Large et al. 1997; Gent et al. 1998) and transient tracer data (Toggweiler et al. 1989a,b; Maier-Reimer 1993; England 1995; Heinze et al. 1998; England and Maier-Reimer 2001). More recently, empirically based methods have been developed for estimating anthropogenic carbon distributions directly from ocean carbon and hydrographic observations (Gruber et al. 1996; Gruber 1998; Wanninkhof et al. 1999; Watson this volume). With the completion of the high quality, JGOFS/WOCE global CO_2 survey (Wallace 1995, 2001), a baseline can be constructed for the world ocean for the pre-industrial DIC field and the anthropogenic carbon perturbation as of the mid-1990s, an invaluable measure for testing numerical model skill and monitoring future evolution.

As an example of this class of carbon uptake simulations, the large-scale patterns of anthropogenic CO_2 air-sea flux and integrated water column inventory from the NCAR CSM Ocean Model (Large et al. 1997; Gent et al. 1998) are shown in Fig. 9.2. The regions of highest anthropogenic carbon uptake – equatorial upwelling bands, western boundary currents, high latitude intermediate and deep water formation regions – are associated with the transport of older subsurface waters to the air-sea interface (Doney 1999). Although the maximum specific uptake rates are found in the subpolar North Atlantic, the area is relatively small, and the integrated uptake of the Southern Ocean and Equatorial band are larger. The anthropogenic DIC water column anomaly is stored primarily in the thermocline and intermediate waters of the subtropical convergence zones and the lower limb of the North Atlantic thermohaline circulation as illustrated by the second panel of Fig. 9.2 and Fig. 9.3, a depth vs. latitude comparison of field data derived and model simulated anthropogenic DIC. The two meridional sections follow the thermohaline overturning circulation from the northern North Atlantic to the Southern Ocean and then back to the northern North Pacific. The model simulates in a reasonable fashion the patterns from empirical estimates except perhaps in the subpolar and intermediate depth North Atlantic, which may reflect problems with the model formation of North Atlantic Deep Water (Large et al. 1997).

At present, most numerical models predict a similar net uptake of anthropogenic CO_2 for the 1990s of approximately 2 Pg C yr^{-1} (1 Pg C equals 10^{15} g C) (Orr et al. 2001), a result supported by atmospheric biogeochemical monitoring and a variety of other techniques (Schimel et al. 1995; Keeling et al. 1996; Rayner et al. 1999). The models, however, show considerable regional differences, particularly in the Southern Ocean (Orr et al. 2001). The agreement of the NCAR model with empirical basin inventories is quite good (Table 9.1), suggesting that at least at this scale the NCAR model transport is relatively skillful.

While based on a more complete description of ocean physics, the coarse resolution, global GCMs used for these carbon studies still require significant parameterization of sub-gridscale phenomenon such as deep wa-

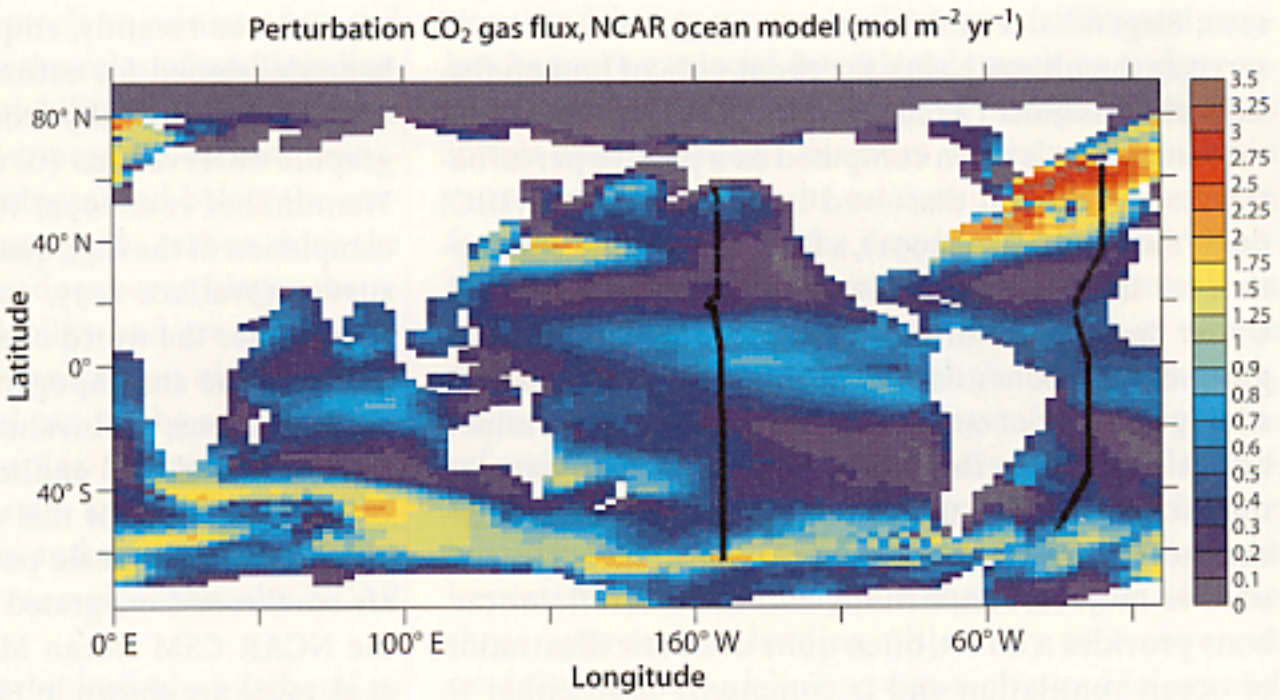

Fig. 9.2.
Spatial distributions of model simulated ocean anthropogenic (perturbation) carbon. Simulated fields are shown for (*top*) air-sea flux (mol C m^{-2} yr^{-1}) and (*bottom*) water column inventory (mol C m^{-2}) for 1990 from the NCAR CSM Ocean Model. The two *lines* indicate the Atlantic and Pacific transects used for the horizontal sections in Fig. 9.3 and 9.7

ter formation, surface and bottom boundary layer physics, and mixing rates along and across density surfaces (isopycnal and diapycnal diffusion). The ongoing OCMIP effort is comparing about a dozen current generation global ocean carbon models among themselves and against ocean observations. Completed analysis of OCMIP Phase 1 and early results from Phase 2 demonstrate significant differences among the models in the physical circulation and simulated chlorofluorocarbon (Dutay et al. 2001), radiocarbon, and current and projected future anthropogenic CO_2 fields (Orr et al. 2001). The largest model-model differences and model-data discrepancies are found in the Southern Ocean, reflecting differences in the relative strength and spatial patterns of Antarctic Mode (Intermediate) Waters and Antarctic Bottom Water (AABW) (Dutay et al. 2001). Models using horizontal mixing rather than an isopycnal scheme (Gent and McWilliams 1990) tend to overestimate convective mixing in the region of the Antarctic Circumpolar Current (Danabasoglu et al. 1994). Not surprisingly, the formation of AABW appears quite sensitive to the under-ice, surface freshwater fluxes in the deep water formation zones (Doney and Hecht 2002); ocean models without active sea ice components appear to have weak AABW formation while many of the interactive ocean-sea ice models tend to have way too much bottom water production.

These known deficiencies in ocean GCM physics hamper quantitative model-data comparisons of biogeochemical and ecosystem dynamical models as well. Uncertainties in the physical flow field, particularly vertical velocity (Harrison 1996), mixing and convection, affect a variety of biogeochemical processes – nutrient supply, boundary layer stability and mean light levels, downward transport of transient tracers, anthropogenic carbon and semi-labile dissolved organic matter – and thus obscure the validation of tracer and biogeochemical components. The refinement of global ocean GCMs is an on-going process, and substantial progress will likely arise from improved treatments of surface boundary forcing and subgrid-scale physics (McWilliams 1996; Haidvogel and Beckmann 1999; Griffes et al. 2000). Transient tracers and biogeochemistry can contribute in this regard by providing additional, often orthogonal, constraints on model performance to traditional physical measures (Gnanadesikan 1999; Gnanadesikan and

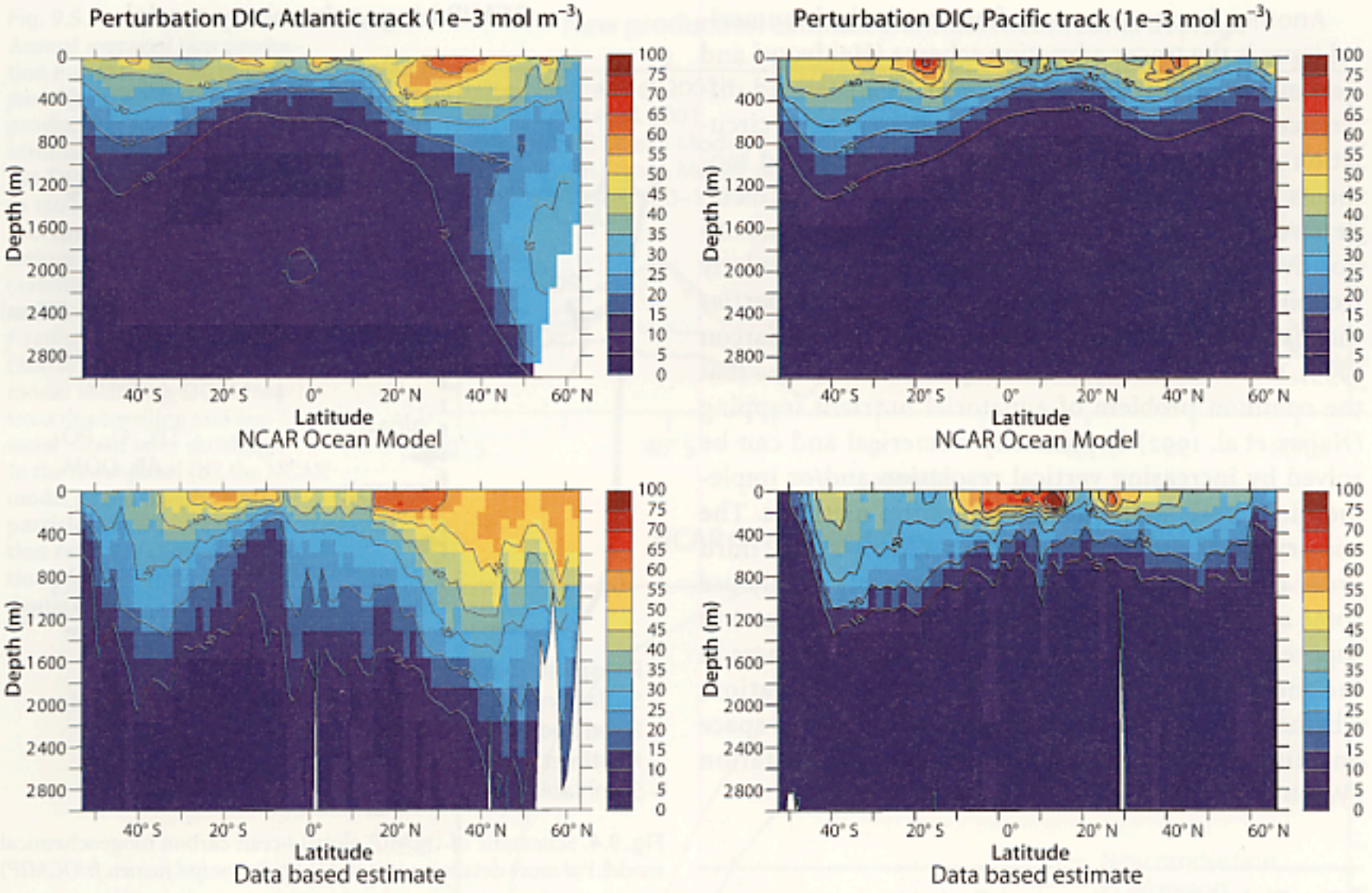

Fig. 9.3. Depth vs. latitude contour plots of anthropogenic CO_2 (mmol C m^{-3}). The panels show the simulated results from the NCAR CSM ocean model and the empirical, observation based estimates (N. Gruber 2000, pers. comm.) each for an Atlantic and Pacific section along the main path of the thermohaline circulation (see Fig. 9.2). Note that depth is limited to 3000 m

Table 9.1.
Estimated basin inventories of anthropogenic DIC (Pg C)

Ocean	NCAR CSM ocean model	Data-based C* estimates	Data reference
Indian	22.1	20 ±3	Sabine et al. (1999)
Atlantic	39.5	40 ±6	Gruber (1998)
Pacific	46.7	46 ±5?	Feely and Sabine (pers. comm.)
Total	108.4	106 ±8?	Feely and Sabine (pers. comm.)

Toggweiler 1999). The incorporation of active biology tests new facets of the physical solutions, especially the surface air-sea fluxes and boundary layer dynamics (Large et al. 1994; Doney 1996; Doney et al. 1998) and their interaction with the interior mesoscale field (Gent and McWilliams 1990).

The desired horizontal resolution for ocean carbon cycle models is often a contentious issue, involving tradeoffs between model fidelity/realism and computational constraints. Most global climate models used for long integrations (i.e., the multi-decade to centennial and longer timescales often of interest to the ocean carbon community) have relatively coarse horizontal resolution of one to a few degrees and thus do not explicitly represent key processes such as deep-water overflows and mesoscale eddies. Increasing the resolution of this class of models is an important objective but is not a general panacea for a number of reasons. First, computational costs increase dramatically; for every factor of two increase in horizontal resolution, the integration time goes up by roughly a factor of 8. Basin-scale, eddy-resolving biological simulations at such resolution are only now becoming computationally feasible and only for short integrations. Second, very high resolution on the order of 1/10° appears to be required to correctly capture the dynamics (not just presence) of the mesoscale eddies (e.g., eddy kinetic energy; eddy-mean flow interactions) (Smith et al. 2000), and some numerical errors persist even as resolution is decreased (Roberts and Marshall 1998). One solution is to incorporate the effect of the unresolved processes using more sophisticated sub-grid scale parameterizations. For example, the Gent and McWilliams (1990) isopycnal mixing scheme tends to greatly reduce the resolution dependence and improves, in both eddy permitting and non-eddy resolving solutions, the simulated meridional heat transport, an important physical diagnostic likely relevant for nutrients and carbon as well as heat.

Another important, and often overlooked, numerical issue is the tracer advection scheme (Haidvogel and Beckmann 1999; Griffes et al. 2000). The centered difference schemes used in most 3-D ocean general circulation models, while conserving first and second moments of the tracer distribution, tend to produce dispersive errors (e.g., under and overshoots, ripples, nonpositive definite tracer fields), which can be particularly troubling for biogeochemical and biological properties that have sharp vertical gradients (Oschlies and Garçon 1999). Oschlies (2000), for example, demonstrates that the common problem of equatorial nutrient trapping (Najjar et al. 1992) is primarily numerical and can be solved by increasing vertical resolution and/or implementing more sophisticated advection methods. The wide range of alternative advection schemes (e.g., third order upwinding, flux corrected transport) mostly use some amount of diffusion (only first order accurate) to suppress the dispersion errors. The main differences in the methods are the magnitude of the dissipation, whether it is applied uniformly or selectively in space and time, and the exact numerical implementation (Webb et al. 1998; Hecht et al. 2000).

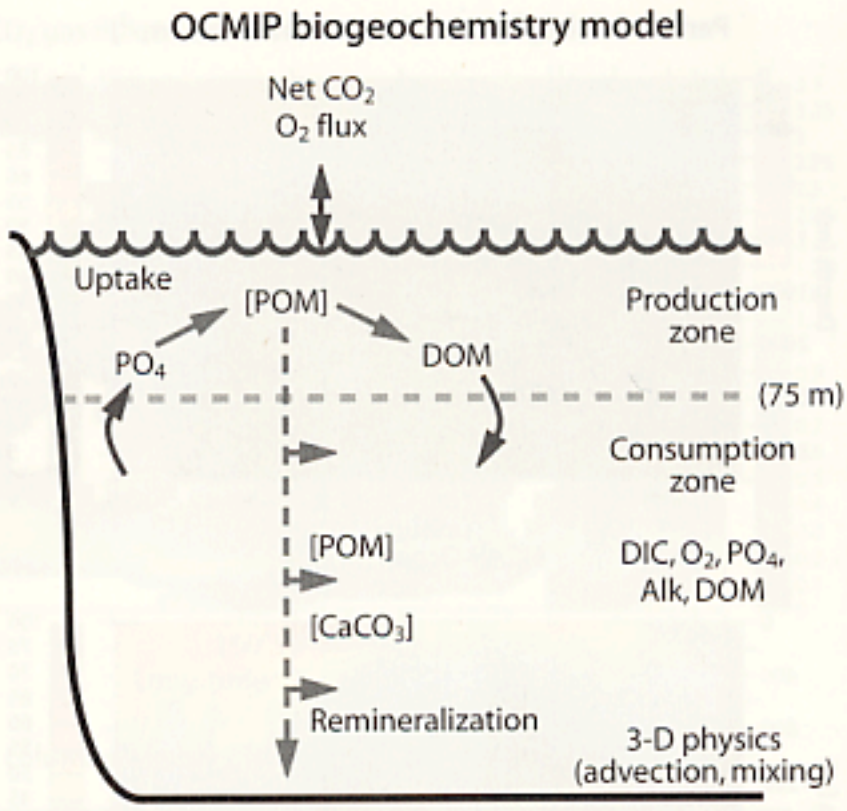

Fig. 9.4. Schematic of OCMIP global ocean carbon biogeochemical model. For more details see text and (*http://www.ipsl.jussieu.fr/OCMIP*)

9.3 Global Biogeochemical Cycles

The net anthropogenic ocean carbon uptake occurs on top of the large background DIC inventory and ocean gradients, air-sea fluxes, biological transformations, and internal transports driven by the natural carbon cycle (Fig. 9.1). Beginning with a series of global biogeochemical simulations in the early 1990s (Bacastow and Maier-Reimer 1990; Najjar et al. 1992; Maier-Reimer 1993), numerical models have played key roles in estimating basin and global-scale patterns and rates of biogeochemical processes (e.g., export production, remineralization). The primary measure for evaluating such models has been the large-scale fields of inorganic nutrients, oxygen, and DIC (Levitus et al. 1993; Conkright et al. 1998; Wallace 2001). As more robust global estimates of biogeochemical rates (e.g., new production, Laws et al. 2000) are developed from the JGOFS field data and satellite remote sensing, they too are being included in model-data comparisons (Gnanadesikan et al. 2001). Numerical biogeochemical models are also valuable tools for exploring specific hypotheses (e.g., iron fertilization; Joos et al. 1991), estimating interannual variability (Le Quéré et al. 2000), and projecting future responses to climate change (Sarmiento et al. 1998).

With a few exceptions (Six and Maier-Reimer 1996), the treatment of biology in these global biogeochemical models to date has been rather rudimentary. This is exhibited in Fig. 9.4 by a schematic of the biotic carbon model from OCMIP Phase 2. The OCMIP model consists of five prognostic variables, a limiting nutrient PO_4, dissolved inorganic carbon DIC, total alkalinity TALK, semi-labile dissolved organic matter DOM, and dissolved oxygen. Upper ocean production (0–75 m) is calculated by restoring excess model PO_4 toward a monthly nutrient climatology (Louanchi and Najjar 2000). The production is split with 1/3 going into rapidly sinking particles and the remainder into the DOM pool. The sinking particles are remineralized in the subsurface consumption zone (>75 m) using an empirical particle flux depth curve similar in form (though with different numerical parameters; Yamanaka and Tajika 1996) to that found by Martin et al. (1987) from sediment trap data. The DOM decays back to phosphate and DIC using first order kinetics with a 6 month time-scale throughout the water column. Most of the DOM is remineralized within the surface production zone but a fraction is mixed or subducted downward prior to decay and thus contributes to overall export production. Surface $CaCO_3$ production is set at a uniform 7% of particulate organic matter production, and all of the $CaCO_3$ is export as sinking particles which are remineralized with a deeper length-scale relative to organic matter. The relative uptake and release rates of PO_4, DIC, and O_2 from the organic pools are set by fixed, so-called Redfield elemental ratios, and CO_2 and O_2 are exchanged with the atmosphere via surface air-sea gas fluxes computed using the quadratic wind-speed gas exchange relationship of Wanninkhof (1992).

Despite its simplicity, the OCMIP model captures to a degree many of the large-scale ocean biogeochemical

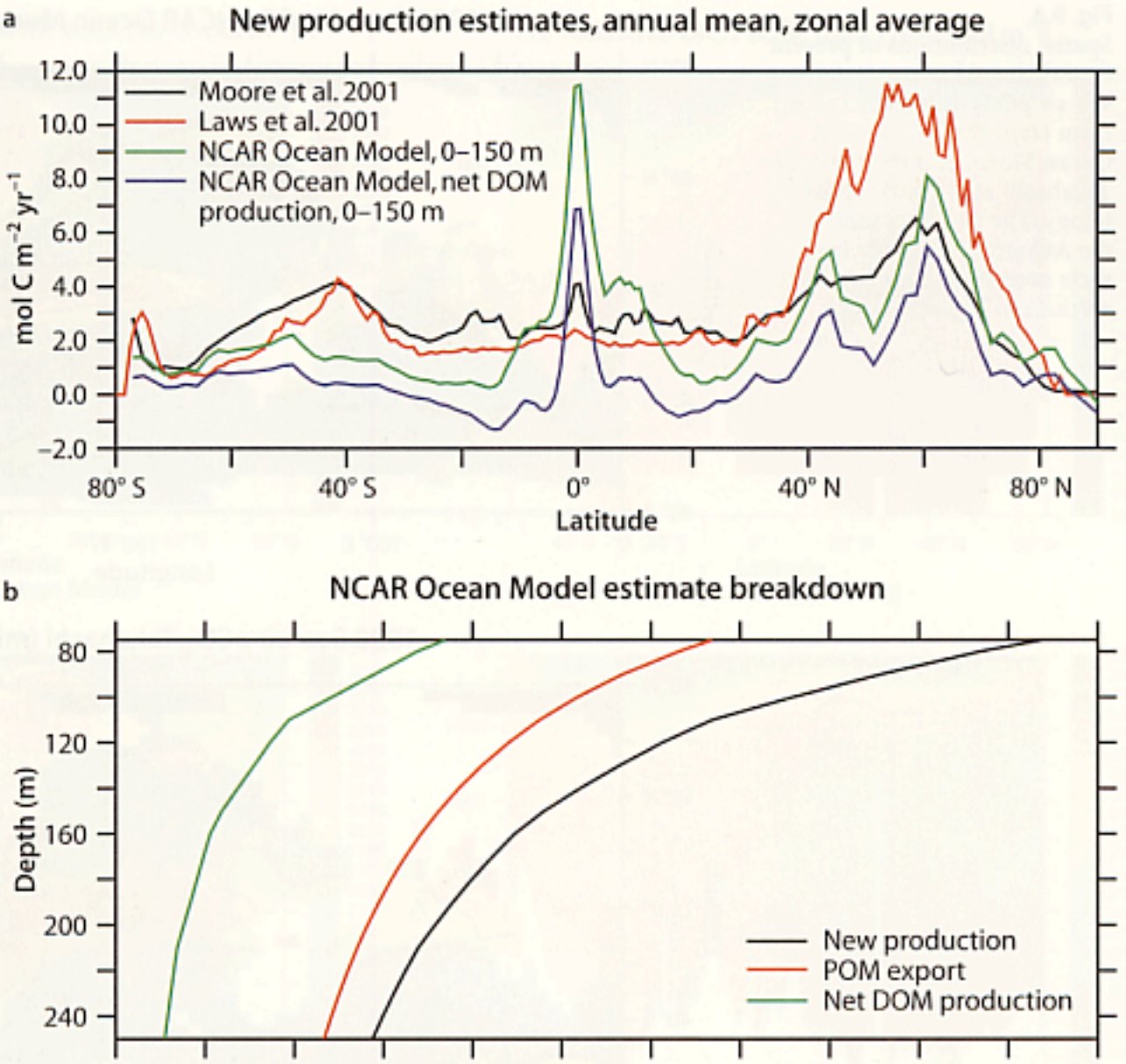

Fig. 9.5.
Annual averaged new production estimates. In the *upper panel* (**a**) the NCAR model total production (particle plus net semi-labile DOM creation) and net DOM creation computed to 150 m are compared against recent new/export production estimates from Laws et al. (2000) (satellite primary production and ecosystem model based *f*-ratios) and Moore et al. (2002a) (global ecosystem model including DOM loss from downwelling and seasonal mixed layer shoaling). In the *lower panel* (**b**), the NCAR model global integral total, particle and DOM new production rates are shown as a function of the bottom limit of the depth integration

patterns found in nature. The model, zonally averaged, total new production (particle export plus net DOM production) is compared in Fig. 9.5a with recent new/export production estimates from Laws et al. (2000) (satellite primary production and ecosystem model based *f*-ratios) and Moore et al. (2002a,b) (global ecosystem model; see below for more details). The NCAR model estimate has been recomputed at 150 m rather than 75 m as specified in the OCMIP formulation to be more consistent with data based and the other model estimates. The global integrated new production estimates from the GCM (9.6 Pg C at 150 m), satellite diagnostic calculation (12.6 Pg C), and ecosystem model (11.9 Pg C) are comparable but with significant regional differences. The Moore et al. and Laws et al. curves have similar patterns with high values in the Northern Hemisphere temperate and subpolar latitudes, low levels in the tropics and subtropics and slightly elevated rates in the Southern Ocean around 40° S. The GCM results are considerably larger in the equatorial upwelling band and lower in the subtropics, reflecting in part net production, horizontal export and subsequent remineralization of organic matter. The Laws et al. (2000) estimates are based on two components: satellite derived primary production rates from CZCS ocean color data and the Behrenfeld and Falkowski (1997) algorithm, and a functional relationship of *f*-ratio to temperature and primary production from an ecosystem model. As discussed by Gnanadesikan et al. (2001), the Laws et al. (2000) values in the equatorial region are sensitive to assumptions about the maximum growth rate as a function of temperature (and implicitly nutrients), and alternative formulations can give higher values.

A significant fraction of the GCM export production at mid- to high latitudes is driven by net DOM production followed by downward transport (global integral at 150 m of 2.4 Pg C) (Fig. 9.5a and 9.5b). This has been observed in the field at a number of locations (Carlson et al. 1994; Hansell and Carlson 1998), and is thought to be an important mechanism north of the Antarctic Polar Front supporting a significant fraction of the organic matter remineralization in the upper thermocline (Doval and Hansell 2000). Because the semi-labile DOM in the model is advected by the horizontal currents, the local sum of new production and remineralization do not always balance leading to regional net convergence/divergence of nutrients and DIC. Some ocean inversion transport estimates, for example, suggest that there are net horizontal inputs of organic nutrients into subtropical areas from remote sources (Rintoul and Wunsch 1991). Another factor to consider when looking at the model production estimates and model-data compari-

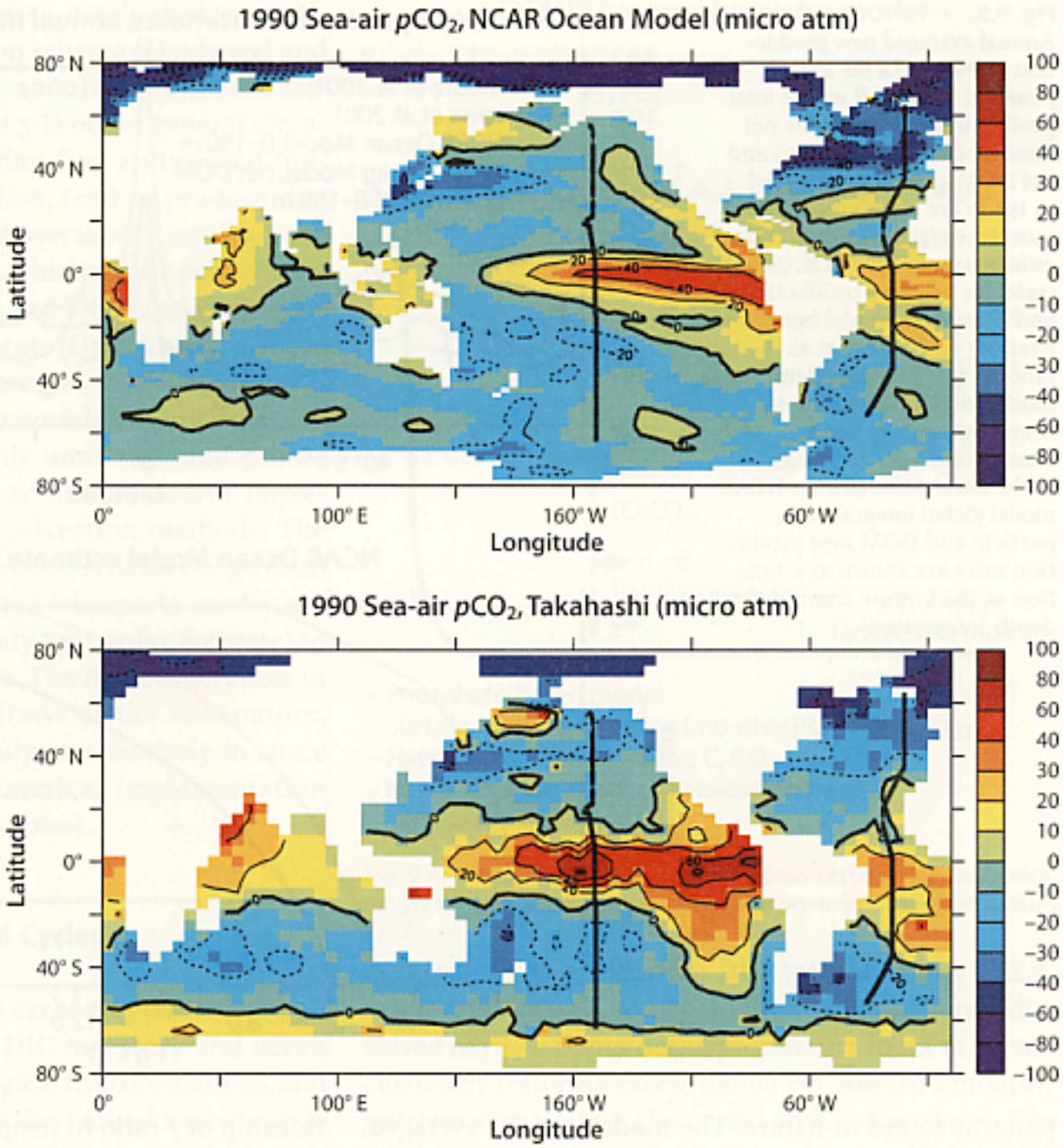

Fig. 9.6.
Spatial distributions of present (1990), annual mean surface sea-air pCO_2 difference (μatm) from (*top*) the NCAR CSM Ocean Model and (*bottom*) the Takahashi et al. (1997) climatology. The two *lines* indicate the Atlantic and Pacific transects used for the horizontal sections in Fig. 9.3 and 9.7

sons is the sensitivity of new production to the depth surface chosen for the vertical integral. The cumulative (surface to depth) new production drops off significantly with depth below 75 m in the model because of the assumed rapid decrease in the sinking particle flux and relatively shallow penetration of DOM governed mostly by seasonal convection (Fig. 9.5b). For most field studies, the vertical mixing and advection terms are difficult to quantify, and the new production is computed typical at either the base of the euphotic zone (100 m to 125 m) or the shallowest sediment trap (~150 m).

Another important measure of model skill is the surface water pCO_2 field (Sarmiento et al. 2000), which can be compared to extensive underway pCO_2 observations (Takahashi et al. 1997, 1999) and atmospheric CO_2 data sets (Keeling et al. 1996; Rayner et al. 1999). The model surface water pCO_2 field is the thermodynamic driving force for air-sea gas exchange and is governed by biological DIC drawdown, physical transport, surface temperature (and salinity), and air-sea fluxes. Figure 9.6 shows the annual mean air-sea ΔpCO_2 field from the model for 1990 (pre-industrial equilibrium plus anthropogenic perturbation) and the Takahashi et al. (1997) climatology. The large-scale patterns are similar with CO_2 outgassing from the equatorial regions, where cold DIC rich water is brought to the surface by upwelling, and CO_2 uptake in the western boundary currents, Antarctic Circumpolar Current, and North Atlantic deep water formation zones. The most striking regional model-data difference is the predicted larger (smaller) model uptake in the Southern Ocean (North Atlantic), compared to the Takahashi et al. (1997) climatology, and the indication of net outgassing right along the Antarctic coast in the observations. Interestingly, the model Southern Ocean results are more in line with recent atmospheric inversion results from the IGBP/GAIM atmospheric transport model intercomparison, TRANSCOM (S. Denning, per. comm. 2000). All three approaches (ocean model, pCO_2 data climatology, and atmospheric inversion) have their own unique uncertainties and potential biases, and more effort should be given to resolving these apparent discrepancies using a combination of improved numerical models and enhanced field data collection.

The model subsurface nutrient, DIC and oxygen fields can also be compared with observations, in this case historical hydrographic data sets and the JGOFS/WOCE global CO_2 survey. The preindustrial DIC results are

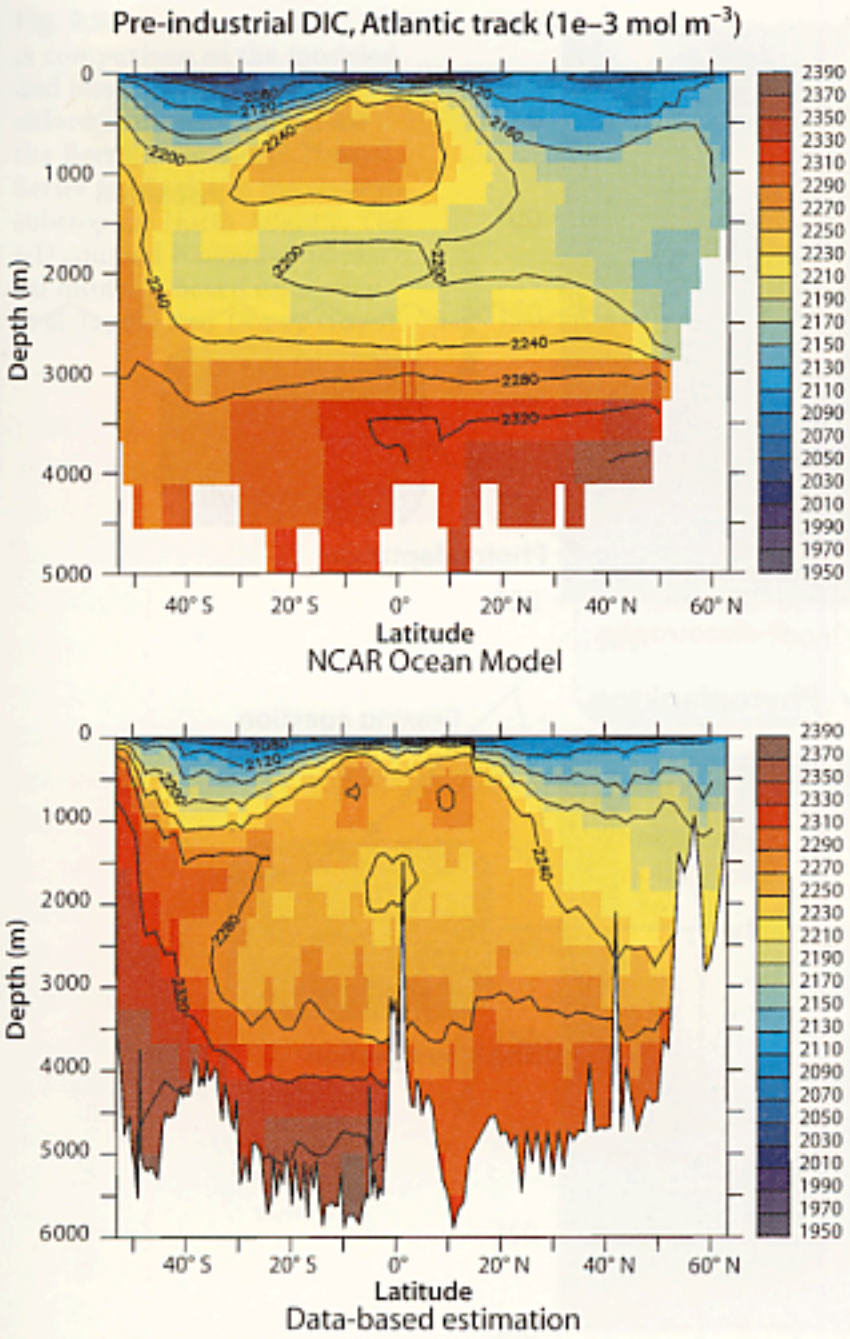

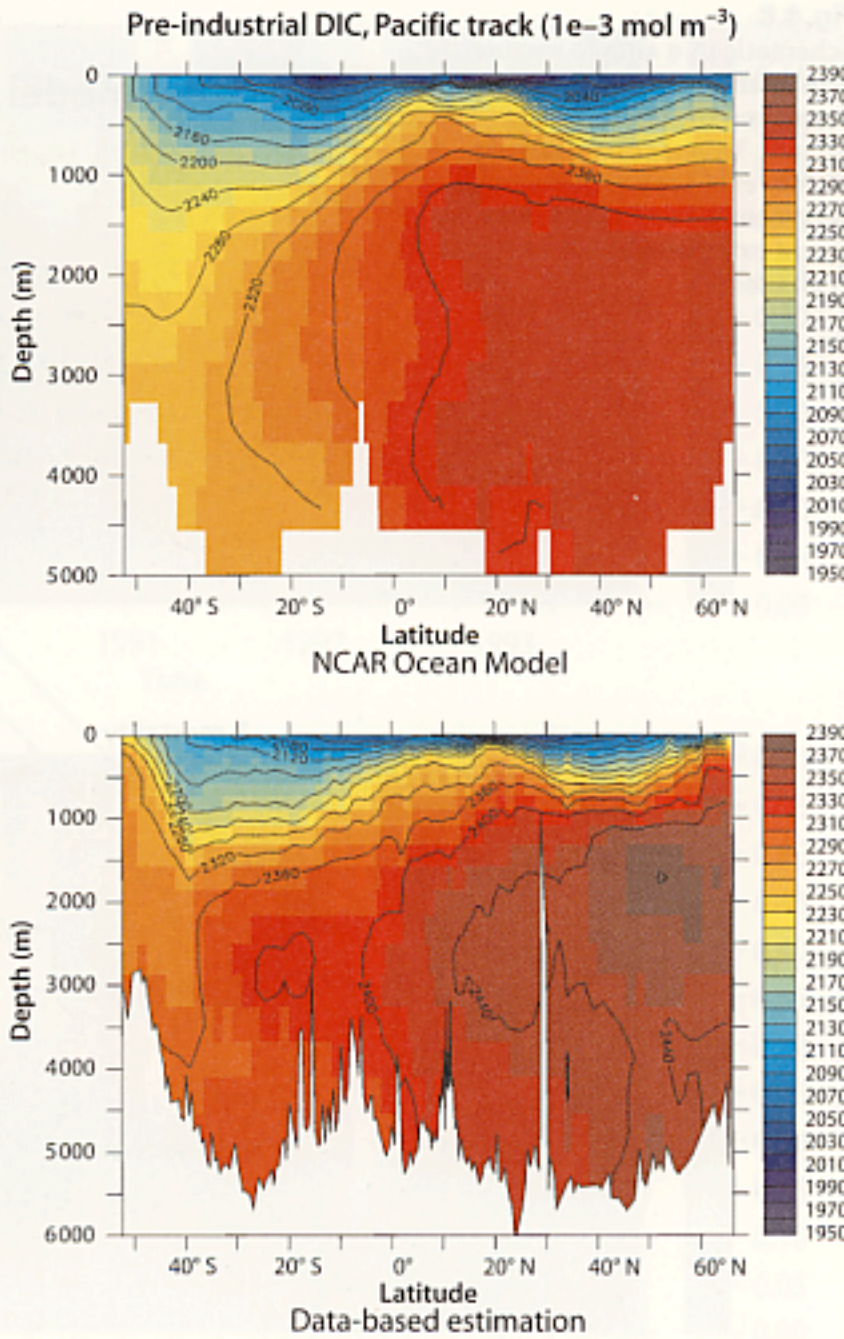

Fig. 9.7. Depth vs. latitude contour plots of pre-industrial DIC (mmol C m^{-3}). The panels show the simulated results from the NCAR CSM ocean model and observed DIC fields with the anthropogenic DIC component removed using the C* technique (N. Gruber 2000, pers. comm.) for an Atlantic and Pacific section along the main path of the thermohaline circulation (see Fig. 9.6)

shown in the same format as for anthropogenic DIC (Fig. 9.3), i.e., meridional sections in the Atlantic and Pacific (Fig. 9.7). The model surface to deep water DIC vertical gradient, which is comparable to the observations, results from contributions of about 2/3 from the biological export ('biological pump') and 1/3 from the physics ('solubility pump'). The horizontal gradients in the deep-water are determined by a mix of the thermohaline circulation and the subsurface particle remineralization rate, and the NCAR-OCMIP model captures most of the broad features. Several of the key model-data differences can be ascribed, at least partly, to problems with the model physics (e.g., too shallow outflow of North Atlantic Deep Water, Large et al. 1997; overly weak production of Antarctic bottom water, Doney and Hecht 2002). The WOCE/JGOFS carbon survey and historical data sets can also be used to estimate the horizontal transport of biogeochemical species within the ocean (e.g., Brewer et al. 1989; Rintoul and Wunsch 1991; Broecker and Peng 1992; Holfort et al. 1998; Wallace 2001), providing another constraint for ocean biogeochemical models (Murnane et al. 1999; Sarmiento et al. 2000; Gruber et al. 2001).

9.4 Ecosystem Dynamics

If the simple OCMIP biogeochemical model captures the zeroth-order state of the ocean carbon cycle then what are the important areas for progress? An obvious deficiency of the OCMIP straw man is the lack of explicit, prognostic biological dynamics to drive surface production, export and remineralization. By linking to a fixed surface nutrient climatology, we have avoided specifying the details of how the surface nutrient field is controlled (e.g., grazing, iron fertilization, mesoscale eddies) or how it might evolve under altered forcing. While useful for the purposes of OCMIP, clearly a more mechanistic approach is desired for many applications. For example, looking toward the next several centuries, future changes in ocean circulation and biogeochemistry may lead to large alterations in the background carbon cycle that could strongly impact projected ocean carbon sequestration (Denman et al. 1996; Sarmiento et al. 1998; Doney and Sarmiento 1999; Boyd and Doney 2003). Realistic projections will require coupled ecosys-

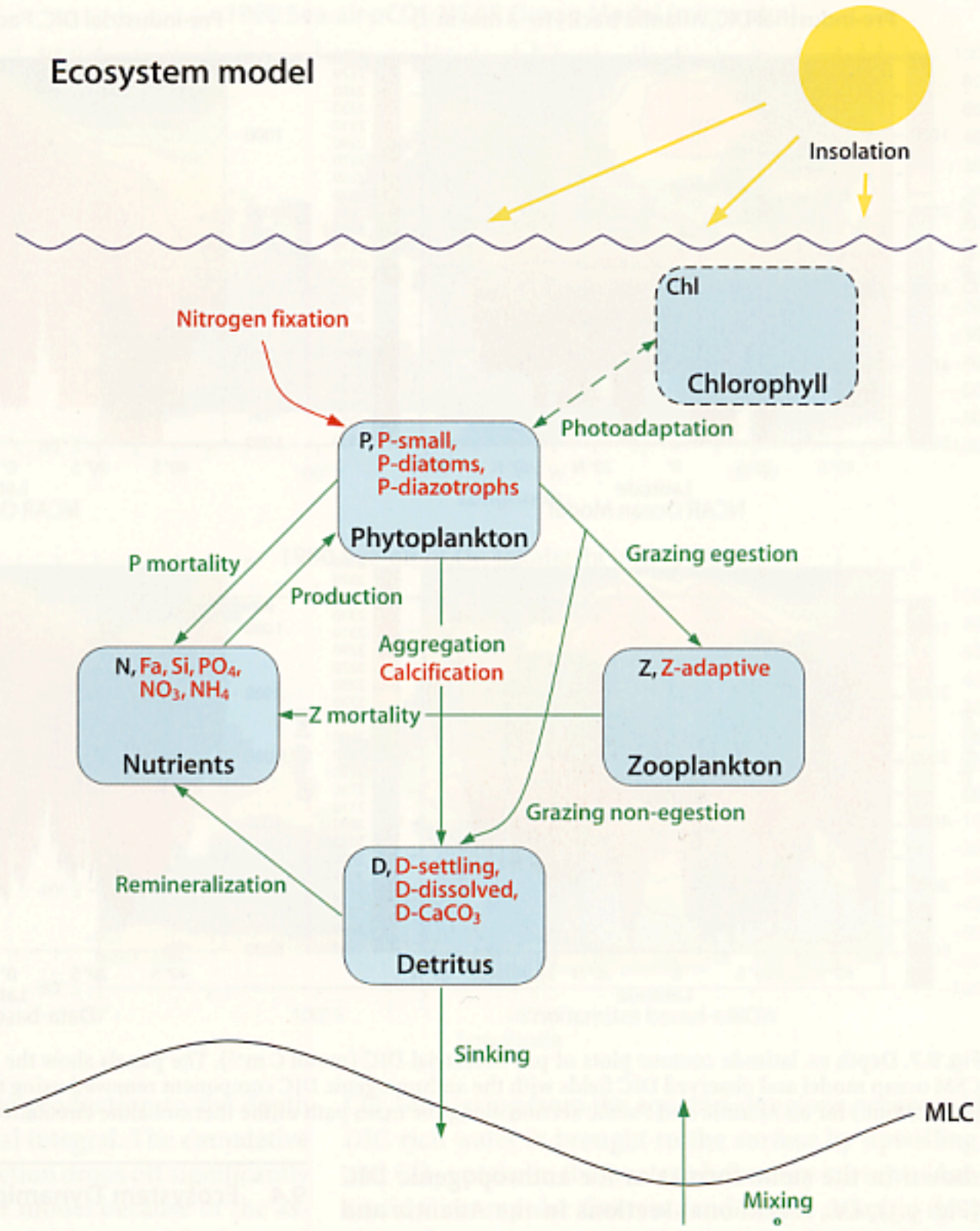

Fig. 9.8.
Schematic of a simple marine ecosystem model originally developed for the Bermuda Atlantic Time-Series Study site (Doney et al. 1996; Doney et al., pers. comm.) and (in *red*) the recent extension by Moore et al. (2001a)

tem-biogeochemical models that include the main processes thought to be sensitive to climate change (e.g., atmospheric dust, nitrogen fixation, community structure).

As an example of a typical marine ecosystem, consider the schematic shown in Fig. 9.8. The model developed for vertical 1-D simulations of the Sargasso Sea by Doney et al. (1996) incorporates five prognostic variables: phytoplankton, zooplankton, nutrient, detritus and chlorophyll (a so-called PZND model). As is common, the model aggregates populations and species of organisms into broadly defined trophic compartments. The equations are based on the flow of a single limiting currency, in this case the concentration of nitrogen (mol N m^{-3}), among compartments rather than individual organisms. The various source/sink terms (e.g., photosynthesis, zooplankton grazing, detrital remineralization) are calculated using standard, though not always well agreed upon, sets of empirical functional forms and parameters derived either from limited field data or laboratory experiments, the latter often with species and conditions of limited relevance to the actual ocean (Fasham 1993; Evans and Fasham 1993; Evans and Garçon 1997). This type of compartment ecosystem model has been used extensively in oceanography (Steele 1974) and theoretical ecology (May 1973; Case 2000) since the early 1970s but has roots much further back in the literature (e.g., Riley 1946; Steele 1958). The area was revitalized about the time of the inception of JGOFS by the seminal work of Evans and Parslow (1985), Frost (1987), Fasham et al. (1990), and Moloney and Field (1991).

Despite its simplifications, the PZND model (Fig. 9.8) does an adequate job capturing the vertical structure and broad seasonal patterns of bulk biogeochemical properties in Bermuda field data (e.g., chlorophyll – Fig. 9.9; nitrate; Doney et al. 1996). Specific features include: a winter phytoplankton bloom following nutrient injection via deep convection; low surface nutrients and chlorophyll during the stratified summer period; and the formation of a sub-

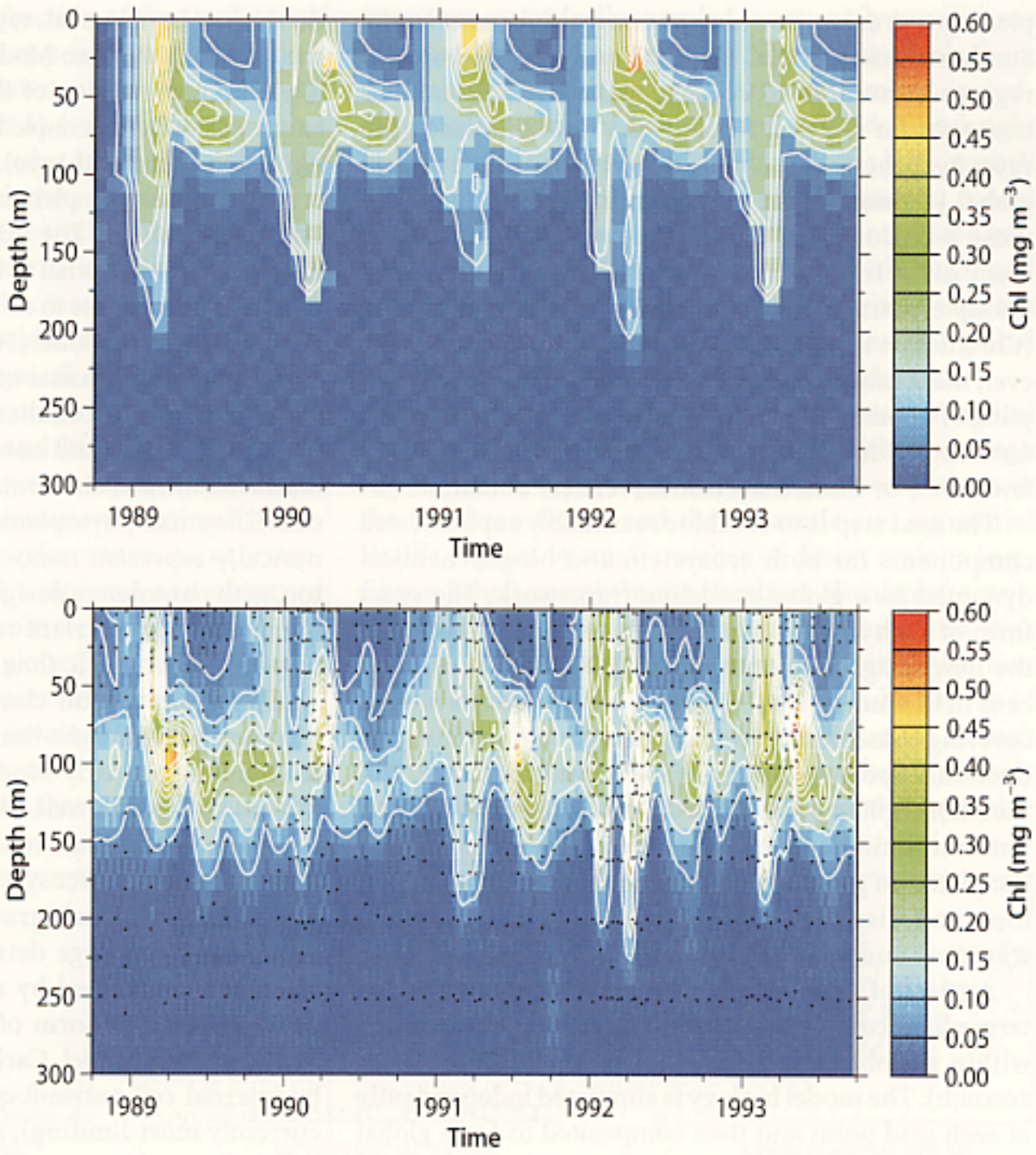

Fig. 9.9.
A comparison of the modeled and observed time-depth chlorophyll distribution for the Bermuda Atlantic Time-Series Study site in the western subtropical North Atlantic. The 1-D coupled biological-physical model is based on Doney et al. (1996) and Doney (1996)

surface chlorophyll maximum at the top of the nutricline. The 1-D coupled biological-physical model, based on surface forcing and physics described by Doney (1996), also reproduces aspects of the observed interannual variability driven by the depth of the winter convection.

Variants on the PZND theme have been successfully applied in vertical 1-D form in a diverse range of biogeographical regimes from oligotrophic subtropical gyres (Bissett et al. 1994) to seasonal bloom regimes (Fasham 1995) to subarctic high-nitrate, low chlorophyll regions (McClain et al. 1996; Pondaven et al. 2000). The construction of the 1-D physical framework (vertical mixing, temperature etc.) requires explicit consideration (Archer 1995; Doney 1996; Evans and Garçon 1997), but in general 1-D coupled models have resulted in useful test-beds for exploring ecological processes and implementing biological data assimilation techniques. It has been known for a while that the relatively simple PZND dynamics belie the ecological complexity of the real system, and recent idealized and local 1-D coupled models include increasing levels of ecological sophistication. Models are incorporating a range of factors such as: size and community structure (Armstrong 1994, 1999a; Bissett et al. 1999), iron limitation (Armstrong 1999b; Leonard et al. 1999; Denman and Pena 1999; Pondaven et al. 2000), and nitrogen fixation (Hood et al. 2001; Fennel et al. 2002). One problem, however, is that most 1-D coupled models are developed and evaluated for a single site, and the generality of these models and their derived parameter values for basin and global simulations remains an open question.

Early three-dimensional basin and global scale calculations (Sarmiento et al. 1993; Six and Maier-Reimer 1996) were conducted with single, uniform PZND ecosystem models applied across the entire domain. These experiments demonstrated that large-scale features such as the contrast between the oligotrophic subtropical and eutrophic subpolar gyres could be simulated qualitatively. Some problems arose, however, with the details. For example, the incorporation of the Fasham et al. (1990) model into a North Atlantic circulation model by Sarmiento et al. (1993) showed too low production and biomass in the oligotrophic subtropics and too weak a spring bloom at high latitudes. The Six and Maier-Reimer (1996) result required careful tuning of the phytoplankton growth temperature sensitivity and zoo-

plankton grazing in order to control biomass in the Southern Ocean HNLC (high nitrate-low chlorophyll) regions. A number of coupled 3-D ecosystem models now exist for regional (Chai et al. 1996; McCreary et al. 1996; Ryabchenko et al. 1998; Dutkiewicz et al. 2001) and global (Aumont et al., pers. comm.) applications, and these 3-D ecosystem models are beginning to include many of the features already addressed in 1-D, including multiple nutrient limitation and community structure (Christian et al. 2001a,b; Gregg et al. 2002). Often, however, these models are not used to fully explore the coupling of upper ocean biology and subsurface carbon and nutrient fields because of the short integration time (a few years) or limited horizontal/vertical domain.

The next step is to combine reasonably sophisticated components for both ecosystem and biogeochemical dynamics in a global modeling framework. The exact form of such a model is yet to be determined. Based on the new insights emerging from JGOFS and other recent field studies, a minimal model can be envisioned covering those basic processes that govern surface production, export flux, subsurface remineralization, and the (de)coupling of carbon from macronutrients (multi-nutrient limitation; size structure and trophic dynamics; plankton geochemical functional groups; microbial loop and dissolved organic matter cycling; particle transport and remineralization).

As part of such a project, we have developed an intermediate complexity, ecosystem model incorporated within a global mixed layer framework (Moore et al. 2002a,b). The model biology is simulated independently at each grid point and then composited to form global fields. The model has a low computational overhead, and thus can be used for extensive model evaluation and exploration. Sub-surface nutrient fields are from climatological databases, and the mixed layer model captures the local processes of turbulent mixing, vertical advection at the base of the mixed layer, seasonal mixed layer entrainment/detrainment, but not horizontal advection. Other forcings include sea surface temperature, percent sea ice cover, surface radiation, and the atmospheric deposition of iron (Fung et al. 2000; Fig. 9.10). The physical forcings are prescribed from climatological databases (Levitus et al. 1994; Conkright et al. 1998) and the NCAR CSM Ocean Model (NCOM) (Large et al. 1997). A preliminary version of the ecosystem model also has been tested in a fully coupled, 3-D North Atlantic Basin configuration (Lima et al. 1999), and the full ecosystem model is currently being implemented in the new global NCAR-Los Alamos model. The mixed layer ecosystem model is discussed in some detail to highlight new modeling directions and approaches to model-data evaluation.

The ecosystem model (Fig. 9.8) is adapted from Doney et al. (1996) and consists of eleven main compartments: small phytoplankton, diatoms, and diazotrophs; zooplankton; sinking and non-sinking detrital classes; and dissolved nitrate, ammonia, phosphorus, iron, and silicate. The small phytoplankton size class is meant to generically represent nano- and pico-sized phytoplankton, with parameters designed to replicate the rapid and highly efficient nutrient recycling found in many subtropical, oligotrophic (low nutrient) environments. The small phytoplankton class may be iron, phosphorus, nitrogen, and/or light-limited. The larger phytoplankton class is explicitly modeled as diatoms and may be limited by silica as well. Many of the biotic and detrital compartments contain multiple elemental pools to track flows through the ecosystem. The model has one zooplankton class which grazes the three phytoplankton groups and the large detritus. Phytoplankton growth rates are determined by available light and nutrients using a modified form of the Geider et al. (1998) dynamic growth model. Carbon fixation rate is governed by internal cell nutrient quotas (whichever nutrient is currently most-limiting), and the cell quotas computed relative to carbon are allowed to vary dynamically as the phytoplankton adapt to changing light levels and nutrient availability. There is good laboratory evidence for a relationship between cell quotas (measured as nutrient/C ratios) and specific growth rates (Sunda and Huntsman 1995; Geider et al. 1998). Photoadaptation is modeled according to Geider et al. (1996, 1998) with a dynamically adaptive Chl/C ratio. The diazotrophs are assumed to fix all required nitrogen from N_2 gas following Fennel et al. (2002) and are limited by iron, phosphorus, light or temperature. Calcification is para-

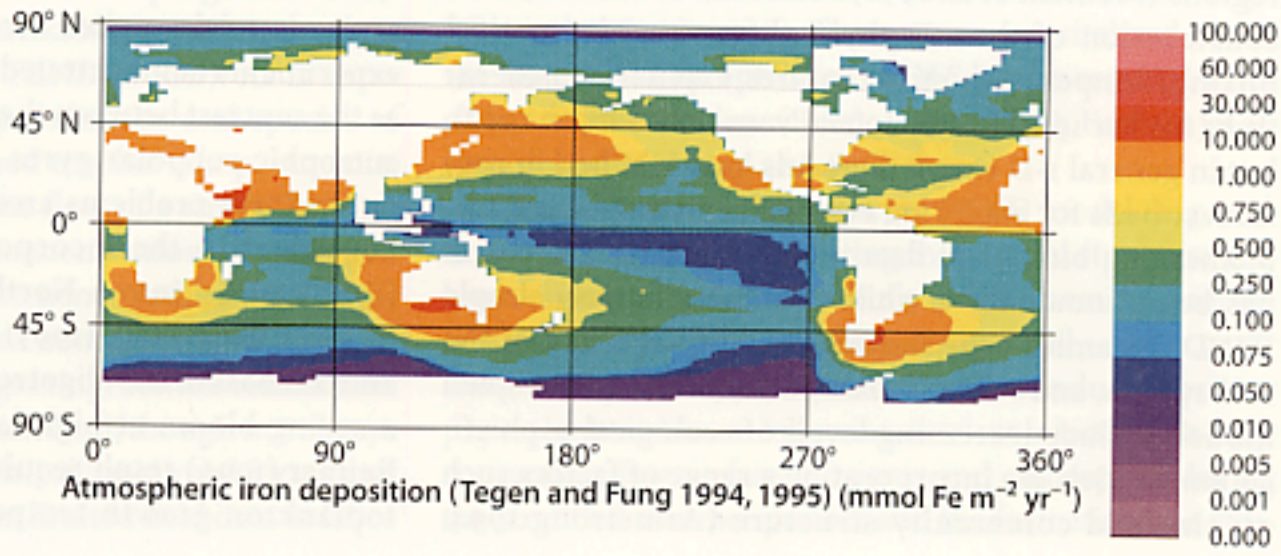

Fig. 9.10. Annual mean map of atmospheric iron deposition to the ocean adapted from Tegen and Fung (1995) model estimates (reprinted from Deep-Sea Res II 49, Moore et al. (2002) Iron cycling and nutrient limitation patterns in surface waters of the world ocean. pp 463–507, © 2002, with permission from Elsevier Science)

meterized as a time-varying fraction of the small (pico/nano) plankton production as a function of ambient temperature and nutrient concentrations. Based on Harris (1994) and Milliman et al. (1999) we assume that grazing processes result in substantial dissolution of $CaCO_3$ in the upper water column.

The model output is in generally good agreement with the bulk ecosystem observations (e.g., total biomass; productivity; nutrients) across diverse ecosystems that include both macro-nutrient and iron-limited regimes and very different physical environments from high latitude sites to the mid-ocean gyres. The detailed, local data sets from JGOFS and historical time-series stations (Kleypas and Doney 2001) have been important for developing parameterizations, testing hypotheses, and evaluating model performance. As an example, a comparison of model simulated and observed mixed layer seasonal cycle for nitrate is shown in Fig. 9.11 for nine locations across the globe. The time-series stations and regional JGOFS process studies (e.g., EqPAC, Arabian Sea) often provide invaluable constraints on biological fluxes (primary productivity profiles, export flux, zooplankton grazing, not shown) as well, parameters that are typically sampled too sparsely to construct global data sets. The variables that are available from observations on a global scale are more limited, including seasonal (now monthly) nutrient fields (Conkright et al. 1998), satellite remotely sensed surface chlorophyll (McClain et al. 1998) (Fig. 9.12) and diagnostic model derived products such as satellite based integrated primary production (Behrenfeld and Falkowski 1997) and *f*-ratio (Laws et al. 2000) estimates. Compared with the satellite estimates, the model produces realistic global patterns of both primary and export production.

The incorporation of iron limitation plays a critical part in the model skill of reproducing the observed high nitrate and low phytoplankton biomass conditions in the Southern Ocean and the subarctic and equatorial Pacific regions. A small number of desert regions (e.g., China, Sahel), mostly in the Northern Hemisphere, provide the main sources of atmospheric dust (and thus iron) to the ocean, and the estimated iron deposition rate to oceanic HNLC environments can be orders of magnitude lower than other locations (Fig. 9.10). At such low deposition rates, upwelling of subsurface iron likely contributes a significant fraction of the total bioavailable

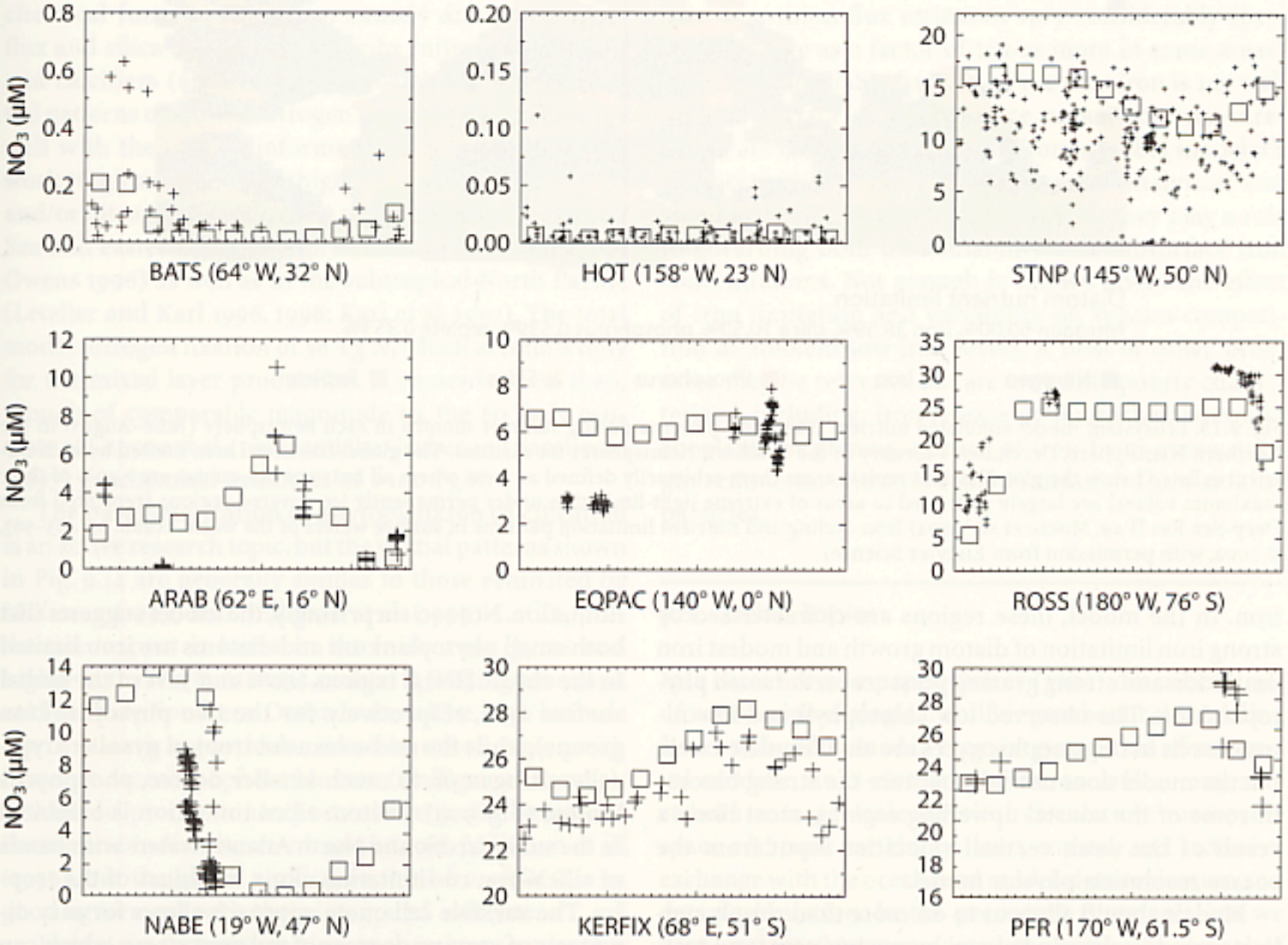

Fig. 9.11. Comparison of simulated and observed seasonal nitrate cycle at nine JGOFS time-series stations across a range of biogeographical regimes (Kleypas and Doney 2001). The model results are from a global mixed layer ecosystem model with uniform biological coefficients (reprinted from Deep-Sea Res II 49, Moore et al. (2002) An intermediate complexity marine ecosystem model for the global domain. pp 403–462, © 2002, with permission from Elsevier Science)

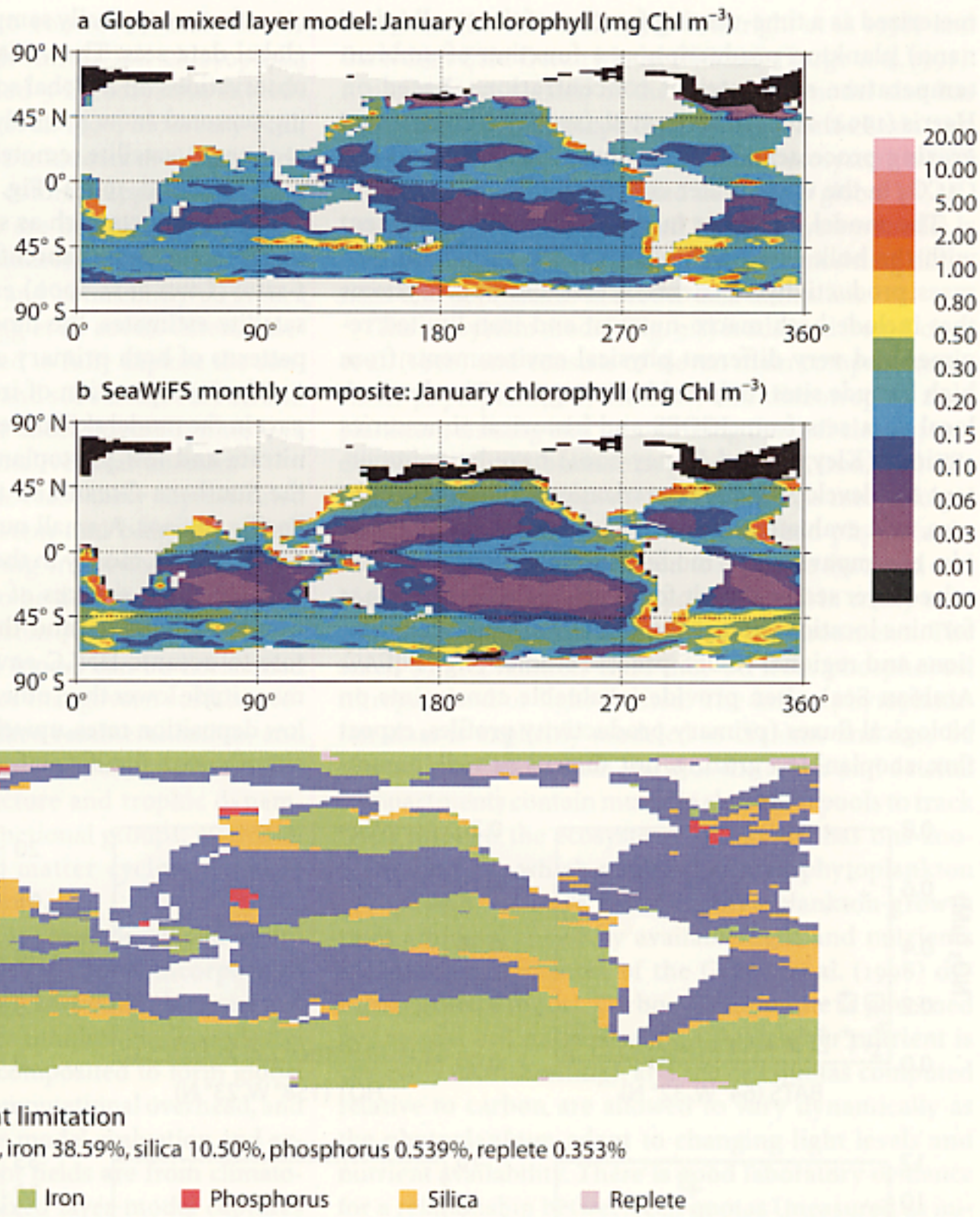

Fig. 9.12. Global field of monthly mean surface chlorophyll concentration for January from SeaWiFS and a global mixed layer ecosystem model (reprinted from Deep-Sea Res II 49, Moore et al. (2002) Iron cycling and nutrient limitation patterns in surface waters of the world ocean. pp 463–507, © 2002, with permission from Elsevier Science)

Fig. 9.13. Ecosystem model simulated nutrient limitation patterns during summer months in each hemisphere (June–August in the Northern Hemisphere, December–February in the Southern Hemisphere) for diatoms. The global fractional area limited by each nutrient is listed below the plot. Nutrient replete areas (here arbitrarily defined as areas where all nutrient cell quotas are >90% of their maximum values) are largely restricted to areas of extreme light-limitation under permanently ice-covered regions (reprinted from Deep-Sea Res II 49, Moore et al. (2002) Iron cycling and nutrient limitation patterns in surface waters of the world ocean. pp 463–507, © 2002, with permission from Elsevier Science)

iron. In the model, these regions are characterized by strong iron limitation of diatom growth and modest iron limitation and strong grazing pressure on the small phytoplankton. The observed low chlorophyll and low nitrate levels in oligotrophic gyres are also simulated well, but the model does not fully capture the strong blooms in some of the coastal upwelling regions, most likely a result of the weak vertical velocities input from the coarse resolution physics model.

Models should allow us to do more than simply replicate what is already known, by posing new (and testable) hypotheses of how the ocean functions at the system level. As an example, the global mixed layer model predicts the degree and time/space patterns of nutrient limitation. Not too surprisingly, the model suggests that both small phytoplankton and diatoms are iron limited in the classic HNLC regions (40% and 52% of the global surface area, respectively for the two phytoplankton groups), while the mid-ocean subtropical gyres are typically nitrogen or, to much smaller degree, phosphorus limited (Fig. 9.13). Diatom silica limitation is exhibited in the subantarctic and North Atlantic waters with bands of silica-iron co-limitation along the edges of the tropics. The variable cell quota approach allows for easy diagnosis of varying degrees of nutrient stress, which can be compared in the near future with global nutrient stress fields to be derived from the MODIS natural fluorescence measurements (Letelier and Abbott 1996).

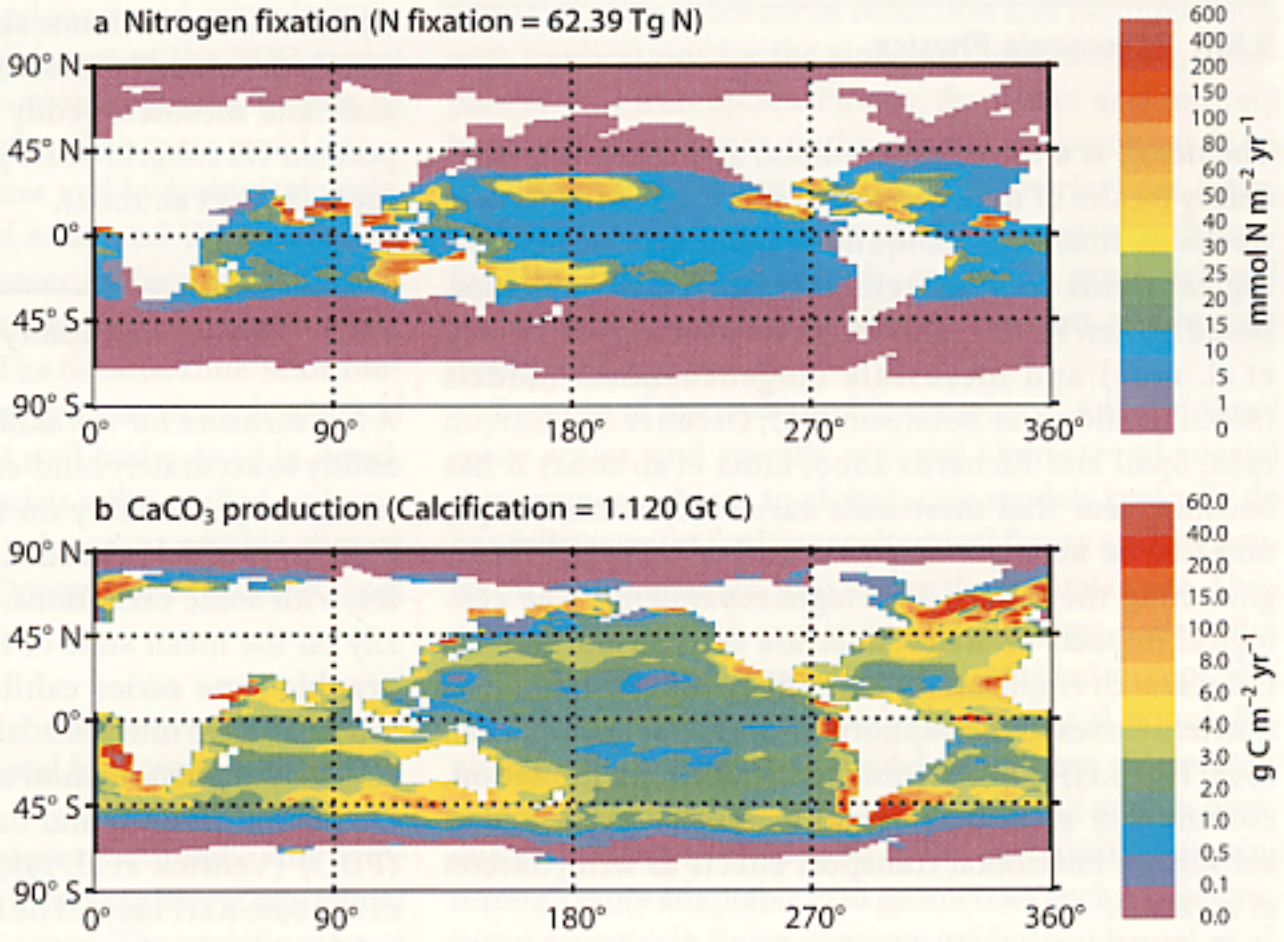

Fig. 9.14. Model simulated annual mean nitrogen fixation and calcification fields (reprinted from Deep-Sea Res II 49, Moore et al. (2002) Iron cycling and nutrient limitation patterns in surface waters of the world ocean. pp 463–507, © 2002, with permission from Elsevier Science)

The other new aspect of the global model is the inclusion of community structure through planktonic geochemical functional groups, namely diatoms (export flux and silica ballast), diazotrophs (nitrogen fixation), and calcifiers (alkalinity and ballast). The model spatial patterns of annual nitrogen fixation (Fig. 9.14) agree well with the limited information known from in situ work (Capone et al. 1997), high trichodesmium biomass and/or nitrogen fixation rates reported in the Caribbean Sea and eastern tropical North Atlantic (Lipschulz and Owens 1996) as well as in the subtropical North Pacific (Letelier and Karl 1996, 1998; Karl et al. 1997). The total model nitrogen fixation of 58 Tg N, which accounts only for the mixed layer production, is somewhat less than, though of comparable magnitude to, the 80 Tg N estimate of Capone et al. (1997) and the Gruber and Sarmiento (1997) geochemical estimates of >100 Tg N.

The parameterization of phytoplankton calcification is an active research topic, but the spatial patterns shown in Fig. 9.14 are generally similar to those estimated by Milliman (1993) and Milliman et al. (1999). $CaCO_3$ production/export is lower in the mid-ocean gyres and higher in the North Atlantic, coastal upwelling zones and mid-latitude Southern Ocean waters. The high latitude North Atlantic in particular is known to be a region with frequent coccolithophore blooms (Holligan et al. 1993). The model production/export is lower in the equatorial Pacific and Indian ocean compared with Milliman et al. (1999), but the global sinking export of 0.46 Gt C is in good agreement with their integrated estimate.

Two main factors limiting progress on ecosystem modeling are the conceptualization of key processes at a mechanistic level and the ability to verify model behavior through robust and thorough model-data comparisons (Abbott 1995). The phytoplankton iron limitation story is an illuminating example. Atmospheric dust/iron deposition flux estimates vary considerably (perhaps as large as a factor of ten or more in some areas) and the bioavailable fraction of the dust iron is not well known. Surface and subsurface ocean iron measurements are limited (particularly from a global modeler's perspective), and there remain serious analytical and standardization issues. Organic ligands may play a role in governing both bioavailability and subsurface iron concentrations. Not enough is known about the effect of iron limitation and variability on species competition at ambient low iron levels. A host of other processes may be relevant, but are currently poorly characterized, including: iron release by photochemistry and zooplankton grazing, release of iron from ocean margin sediments, and iron remineralization from sinking particles.

9.5 Other Topics

In a recent review paper, Doney (1999) described a set of key marine ecological and biogeochemical modeling issues to be addressed in the next generation of numerical models: multi-element limitation and community structure; large-scale physical circulation; mesoscale space and time variability; land, coastal, and sediment exchange with the ocean; and model-data evaluation and data assimilation. In the preceding three sections we have presented in some detail the nature of several of these challenges and specific initial progress made by our group. Below we more briefly outline some of the remaining items.

9.5.1 Mesoscale Physics

The ocean is a turbulent medium, and mesoscale variability (scales of 10 to 200 km in space and a few days to weeks in time) is a ubiquitous feature of ocean biological fields such as remotely sensed ocean color. Based on new in situ measurement technologies (Dickey et al. 1998) and mesoscale biogeochemical models (McGillicuddy and Robinson 1997; Oschlies and Garçon 1998; Spall and Richards 2000; Lima et al. 2002) it has become clear that mesoscale variability is not simply noise to be averaged over, but rather a crucial factor governing the nature of pelagic ecosystems. The ecological impacts of disturbance are diverse, and the initial research emphasis on the eddy enhancement of new nutrient fluxes to the euphotic zone (McGillicuddy et al. 1998; Fig. 9.15) is broadening to include light limitation, community structure, organic matter export, and subsurface horizontal transport effects as well (Garçon et al. 2001).

Quantifying the large-scale effect of such variability will require concerted observational, remote sensing and numerical modeling programs with likely heavy reliance on data assimilation. The computational demands of truly eddy resolving basin to global calculations are significant, however. Recent high resolution physical simulations of the North Atlantic show that dramatic improvement in eddy statistics and western boundary current dynamics is reached only at 1/10 of a degree resolution (Smith et al. 2000), and even higher resolution may be needed for biology if submesoscale (0.5–10 km) processes are as important as suggested by preliminary results (Levy et al. 1999; Mahadevan and Archer 2000; Lima et al. 2002). Over the near term, long time-scale equilibrium and climate simulations will be limited primarily to non-eddy resolving models in which submesoscale and mesoscale eddy effects will have to be incorporated via subgrid-scale parameterizations (Levy et al. 1999; Lima et al. 2002).

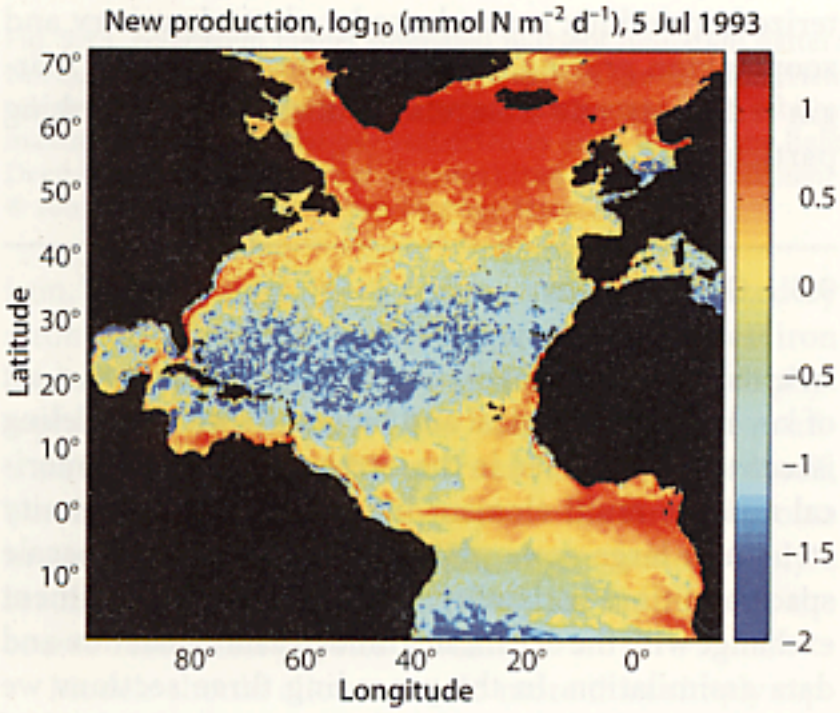

Fig. 9.15. Daily snapshot of new production from a Los Alamos-POP 1/10° mesoscale simulation of the North Atlantic (Dennis McGillicuddy, pers. comm.)

9.5.2 Climate Variability and Secular Change

A key measure for the skill of numerical models is their ability to accurately hind-cast oceanic responses to natural climate variability on timescales from the seasonal cycle to multiple decades. Large-scale modeling studies, with some exceptions, have tended to focus primarily on the mean state of the ocean. Biological oceanographic time series exhibit significant variability on interannual to interdecadal scales associated with physical climate phenomenon such as the El Niño-Southern Oscillation (ENSO) and the Pacific Decadal Oscillation (PDO) (Venrick et al. 1987; Karl et al. 1995; McGowan et al. 1998; Karl 1999). The ecosystem response to physical forcing may be quite nonlinear, manifesting in the North Pacific, for example, as a major biological regime shift in the mid-1970s due to the PDO (Francis and Hare 1994). Comparable climate related biological shifts are also inferred for the North Atlantic (Reid et al. 1998). Retrospective models can help explain the underlying mechanisms of such phenomena (Polovina et al. 1995). Because of an interest in separating terrestrial and oceanic signals in the atmospheric CO_2 network, there is also a growing effort to model the oceanic contribution to atmospheric variability, which appears to be small except for the tropical ENSO signal (Rayner et al. 1999; Le Quéré et al. 2000).

Numerical models are also being used to project the potential marine biogeochemical responses to anthropogenic climate change (Sarmiento et al. 1998; Matear and Hirst 1999). Coupled ocean-atmosphere model simulations differ considerably in their details, but most models suggest general warming of the upper ocean and thermocline, increased vertical stratification in both the low latitude (warming) and high latitude (freshening) surface waters, and weakening of the thermohaline circulation. Combined, the physical effects lead to a 30–40% drop in the cumulative anthropogenic CO_2 uptake over the next century partly compensated by changes in the strength of the natural biological carbon pump. Given the low level of biological sophistication used in these early simulations, such projections must be considered preliminary, demonstrating the potential sensitivity of the system and posing important questions to be addressed through future research.

Preliminary ecosystem simulations (Bopp et al. 2001) show different regional climate change responses to enhanced stratification with decreased subtropical pro-

ductivity (nutrient limited) and increased subpolar productivity (light limited) reminiscent of the PDO signal (Polovina et al. 1995). Other environmental factors to consider include alterations of aeolian trace metal deposition due to changing land-use and hydrological cycle, variations in cloud cover and solar and UV irradiance, coastal eutrophication, and lower surface water pH and carbonate ion concentrations due to anthropogenic CO_2 uptake (Kleypas et al. 1999). The decadal time-scale biogeochemical and ecological responses to such physical and chemical forcings are not well understood in detail, and prognostic numerical models will be relied on heavily along with historical and paleoceanographic climate variability reconstructions (Doney and Sarmiento 1999; Boyd and Doney 2003).

9.5.3 Land, Coastal Ocean, and Sediment Interactions

The coastal/margins zone interacts strongly and complexly with the land, adjacent atmosphere, continental shelves and slopes, and open-ocean. The specific rates of productivity, biogeochemical cycling, and organic/inorganic matter sequestration are higher than those in the open ocean, with about half of the global integrated new production occurring over the continental shelves and slopes (Walsh 1991; Smith and Hollibaugh 1993). The high organic matter deposition to, and close proximity of the water column to, the sediments raises the importance of sedimentary chemical redox reactions (e.g., denitrification, trace metal reduction and mobilization), with implications for the global carbon, nitrogen, phosphorus and iron cycles. Finally, the direct and indirect human perturbations to the coastal environment (e.g., pollution, nutrient eutrophication, fisheries) are large, with important impacts on marine ecosystems (harmful algal blooms, coral reefs, spawning grounds) and society (e.g., commercial fisheries, tourism, and human health and aesthetics).

Because of the topographic complexity, smaller time/space scales, and specific regional character of coastal environments, basin to global scale models typically do not fully account for biogeochemical fluxes and dynamics on continental margins and in the coastal ocean. Thus coastal/open-ocean exchange and the large-scale influence on the ocean are not well quantified except in a few locations (Falkowski et al. 1994; Liu et al. 2000). Regional coastal ecosystem models have been moderately successful (Robinson et al. 2001; Fig. 9.16), and an obvious next step is to meld open ocean and coastal domains through more adaptable grid geometries such as unstructured (spectral) finite element grids (Haidvogel et al. 1997) or by embedding regional domain, higher-resolution models (Spall and Holland 1991). Dynamic marine sediment geochemistry models (Heinze et al. 1999) are needed both for the coastal problem and for large-scale paleoceanographic applications, an example being the compensation of the sediment $CaCO_3$ to changes in ocean carbon chemistry on millennial time-scales (Archer and Maier-Reimer 1994; Archer et al. 2000).

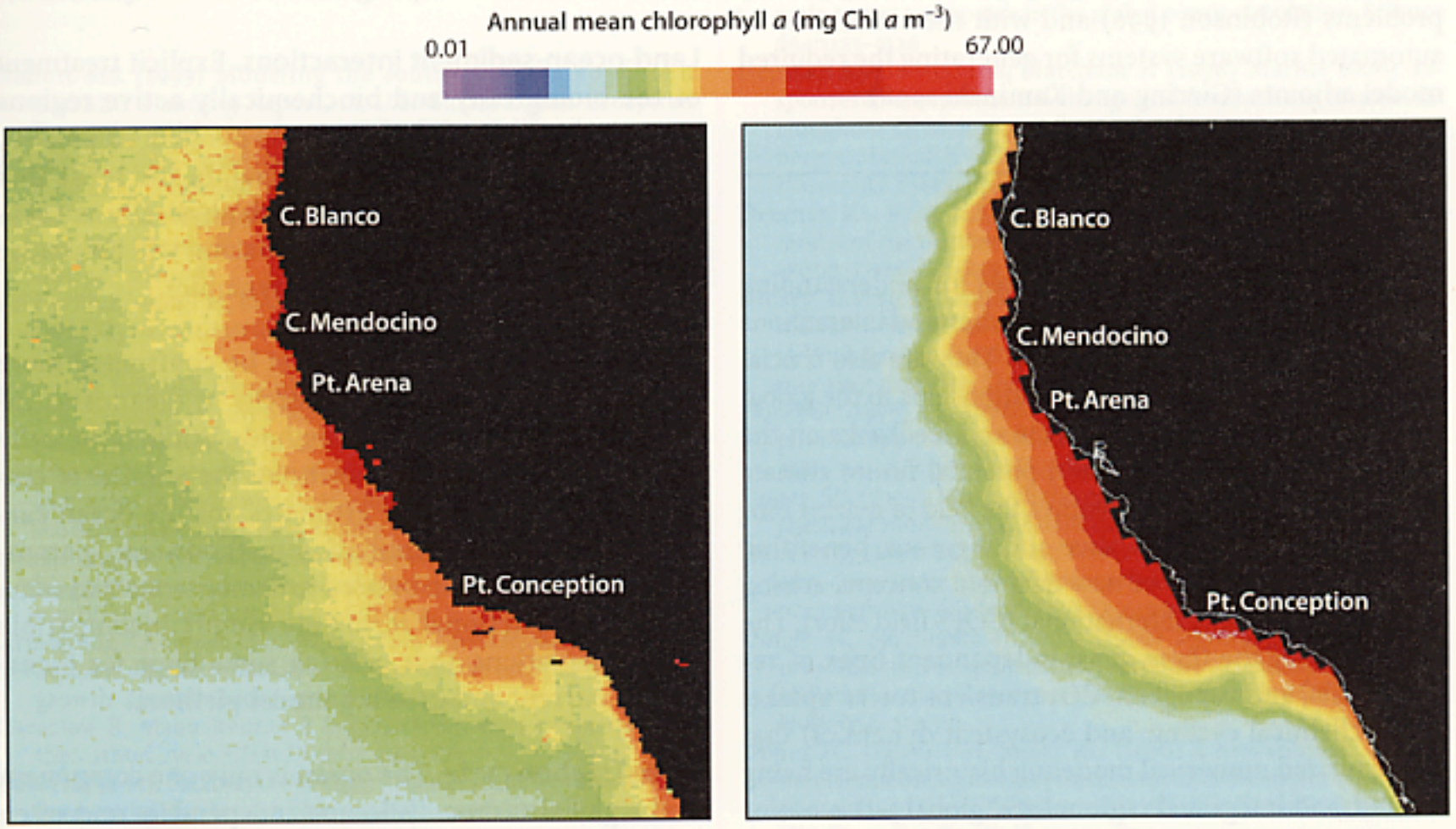

Fig. 9.16. Annual mean chlorophyll for the California Current coastal region from SeaWiFs and the UCLA regional coastal ecosystem model ROMS (James McWilliams, pers. comm.)

9.5.4 Inverse Modeling and Data Assimilation

The emerging techniques of inverse modeling and data assimilation, which more formally compare and meld model results and data, are becoming essential in model development and evaluation (U.S. JGOFS 1992; Kasibhatla et al. 2000). In theory data assimilation provides a solution, if it exists, that is dynamically consistent with both the observations and model equations within the estimated uncertainties. Much of the art of data assimilation lies in assigning relative error weights to different data types and to the model equations themselves, the so-called cost function problem (U.S. JGOFS 1992). A number of recent studies have used this approach to better constrain or optimize parameters for marine biogeochemical box and one-dimensional models, particularly with time series data (Matear 1995; Fasham and Evans 1995; Hurtt and Armstrong 1996; Spitz et al. 1998; Fennel et al. 2001). Applications to three-dimensional models are more limited but include efforts to assimilate satellite ocean color data into ecosystem models (Ishizaka 1990) or to estimate poorly measured fluxes such as dissolved organic phosphorus transport/remineralization (Matear and Holloway 1995), surface export production (Schlitzer 2000), and air-sea oxygen fluxes (Gruber et al. 2001) from the large-scale nutrient distributions and physical circulation flow fields. The utility of data assimilation will continue to grow with the import and refinement of numerical methods from meteorology and physical oceanography to interdisciplinary problems (Robinson 1996) and with the availability of automated software systems for generating the required model adjoints (Giering and Kaminski 1998).

9.6 Summary

Numerical models are essential tools for understanding the complex physical, biological and chemical interactions that govern the ocean carbon cycle. They are also crucial for extrapolating local/regional relationships to the global scale and for projecting the effects and feedbacks on the ocean carbon cycle of past and potential future climate change. As outlined in this chapter, the field of marine biogeochemical modeling is alive and vigorous, benefiting greatly from the surge of new data and concepts arising from the decade long international JGOFS field effort. The boundaries of the three quasi-independent lines of research (i.e., anthropogenic CO_2 transient tracer uptake; biogeochemical cycling; and ecosystem dynamics) that characterized numerical modeling historically are being blurred, and integrated regional and global 3-D eco-biogeochemical models are emerging. These models are based on the new paradigms of multi-element cycling, community structure and geochemical functional groups (e.g., nitrogen fixers, calcifiers), key to addressing hypotheses of how the ocean might alter or drive long term changes in atmospheric CO_2. Growing utilization of retrospective or hindcasting experiments will be used to evaluate model skill relative to historical interannual and paleoclimate variability. Significant progress is also being made in process and regional models on issues such as biological-physical sub- and mesoscale interactions as well as coastal ecosystem and biogeochemical dynamics.

A number of major challenges remain for the next decade(s):

Ecological sophistication. Ocean models must be grounded at a more fundamental level by ecological and evolutionary hypotheses. The current emphasis is often on simulating chemical and biochemical analyses: phytoplankton treated simply as concentrations of pigments and organic carbon, zooplankton as grazers, and physics as a mechanism for providing nutrients. A more mechanistic understanding is needed of how individual organisms and species interact to form pelagic ecosystems, how food webs affect biogeochemical fluxes, and how the structure of food webs and corresponding biogeochemical fluxes will change in the coming decades.

High frequency variability. The importance of high frequency spatial and temporal variability (e.g., fronts, mesoscale eddies) on the large-scale carbon cycle needs to be better characterized. This will require a combination of subgrid-scale parameterizations, nested models, and dedicated very high-resolution computations.

Land-ocean-sediment interactions. Explicit treatment of the biologically and biochemically active regions along continents needs to be incorporated. At present, coastal modeling is often 'parochial' in the sense that each region is treated as unique both physically and ecologically. The computational approaches will be similar to those outlined for mesoscale dynamics.

Model-data fusion. Models must be confronted more directly with data using a hierarchy of diagnostic, inverse, and data assimilation methods. While technically challenging, data assimilation holds the promise of creating evolving, 4-D 'state estimates' for the ocean carbon cycle. Further, assimilation methods (e.g., parameter optimization) can be used to demonstrate that some models or functional forms are simply incompatible with observations, thus offering some hope for focusing the current and growing model plethora.

Global carbon cycle. The ocean is only one component of the global carbon cycle, and independent and often complementary estimates of key measures of ocean carbon dynamics are being developed by scientists working in other disciplines. Examples include air-sea CO_2

fluxes based on atmospheric inversions and seasonal marine net community production based on atmospheric O_2/N_2 ratios. Similar to progress made in ocean-atmosphere modeling, one solution is to emphasize and attempt to reconcile model fluxes that occur between the ocean-atmosphere and land-ocean. Another is to actively pursue adding integrated carbon cycle dynamics into coupled (ocean-atmosphere-land) climate models.

Acknowledgements

We would like to thank our numerous colleagues and collaborators who have contributed to this chapter through formal and informal discussions, comments, and research material. We especially thank P. Falkowski, D. Feely, I. Fung, D. Glover, N. Gruber, J. Kleypas, I. Lima, F. Mackenzie, D. McGillicuddy, J. McWilliams, C. Sabine, and S. Smith. We also thank the editor of this volume, M. Fasham, and an anonymous reviewer for providing guidance and suggestions on the text. This work is supported in part by a NASA US Ocean Carbon Model Intercomparison Project (OCMIP Phase II) grant (NASA W-19,274), a NOAA-OGP Global Carbon Cycle grant (NOAA-NA96GP0360), and the NSF US JGOFS Synthesis and Modeling Project management grant (NSF 97308). The National Center for Atmospheric Research is sponsored by the US National Science Foundation.

References

Abbott MR (1995) Modeling the southern ocean ecosystem. GLOBEC Planning Report, 18, U.S. Global Ocean Ecosystem Dynamics (GLOBEC) Program, Berkeley, California, 63 pp

Archer D (1995) Upper ocean physics as relevant to ecosystem dynamics: a tutorial. Ecol Appl 5:724–739

Archer D, Maier-Raimer E (1994) Effect of deep-sea sedimentary calcite preservation on atmospheric CO_2 concentration. Nature 367:260–263

Archer D, Kheshgi H, Maier-Reimer E (1998) Dynamics of fossil fuel CO_2 neutralization by marine $CaCO_3$. Global Biogeochem Cy 12:259–276

Archer D, Eshel G, Winguth A, Broecker W (2000) Atmospheric CO_2 sensitivity to the biological pump in the ocean. Global Biogeochem Cy 14:1219–1230

Armstrong RA (1994) Grazing limitation and nutrient limitation in marine ecosystems: steady state solutions of an ecosystem model with multiple food chains. Limnol Oceanogr 39:597–608

Armstrong RA (1999a) Stable model structures for representing biogeochemical diversity and size spectra in plankton communities. J Plankton Res 21:445–464

Armstrong RA (1999b) An optimization-based model of iron-light ammonium colimitation of nitrate uptake and phytoplankton growth. Limnol Oceanogr 44:1436–1446

Bacastow R, Maier-Reimer E (1990) Ocean-circulation model of the carbon cycle. Clim Dynam 4:95–125

Behrenfeld MJ, Falkowski PG (1997) Photosynthetic rates derived from satellite-based chlorophyll concentration. Limnol Oceanogr 42:1–20

Bissett WP, Meyers MB, Walsh JJ (1994) The effects of temporal variability of mixed layer depth on primary productivity around Bermuda. J Geophys Res 99:7539–7553

Bissett WP, Walsh JJ, Carder KL (1999) Carbon cycling in the upper waters of the Sargasso Sea: I. Numerical simulation of differential carbon and nitrogen fluxes. Deep-Sea Res Pt I 46:205–269

Bopp L, Monfray P, Aumont O, Dufresne J-L, Le Treut H, Madec G, Terray L, Orr JC (2001) Potential impact of climate change on marine export production. Global Biogeochem Cy 15:81–99

Boyd P, Doney S (2003) The impact of climate change and feedback process on the ocean carbon cycle. Chap. 7. Springer-Verlag, (this volume)

Brewer PG, Goyet C, Dyrssen D (1989) Carbon dioxide transport by ocean currents at 25° N latitude in the Atlantic Ocean. Science 246:477–479

Broecker WS, Peng T-H (1992) Interhemispheric transport of carbon dioxide by ocean circulation. Nature 356:587–589

Broecker W, Lynch-Stieglitz J, Archer D, Hofmann M, Maier-Reimer E, Marchal O, Stocker T, Gruber N (1999) How strong is the Harvardton-Bear constraint? Global Biogeochem Cy 13:817–820

Capone DG, Zehr JP, Paerl HW, Bergman B, Carpenter EJ (1997) Trichodesmium: a globally significant cyanobacterium. Science 276:1221–1229

Carlson CA, Ducklow HW, Michaels AF (1994) Annual flux of dissolved organic carbon from the euphotic zone in the northwest Sargasso Sea. Nature 371:405–408

Case TJ (2000) An illustrated guide to theoretical ecology. Oxford University Press 4, 49 pp

Chai F, Lindley ST, Barber RT (1996) Origin and maintenance of high nutrient condition in the equatorial Pacific. Deep-Sea Res Pt II 42:1031–1064

Christian JR, Verschell MA, Murtugudde R, Busalacchi AJ, McClain CR (2001a) Biogeochemical modelling of the tropical Pacific Ocean. I. Seasonal and interannual variability. Deep-Sea Res Pt II 49:509–543

Christian JR, Verschell MA, Murtugudde R, Busalacchi AJ, McClain CR (2001b) Biogeochemical modelling of the tropical Pacific Ocean. II. Iron biogeochemistry. Deep-Sea Res Pt II 49:545–563

Conkright ME, Levitus S, O'Brien T, Boyer TP, Stephens C, Johnson D, Stathoplos L, Baranova O, Antonov J, Gelfeld R, Burney J, Rochester J, Forgy C (1998) World ocean atlas database 1998 CD-ROM data set documentation. National Oceanographic Data Center, Silver Spring, MD

Danabasoglu G, McWilliams JC, Gent PR (1994) The role of mesoscale tracer transports in the global ocean circulation. Science 264:1123–1126

Denman K, Hofmann E, Marchant H (1996) Marine biotic responses to environmental change and feedbacks to climate. In Houghton JT, Meira LG Filho, Callander BA, Harris N, Kattenberg A, Maskell K (eds) Climate change 1995. IPCC, Cambridge University Press, pp 487–516

Denman KL, Pena MA (1999) A coupled 1-D biological/physical model of the northeast subarctic Pacific Ocean with iron limitation. Deep-Sea Res Pt II 46:2877–2908

Dickey T, Frye D, Jannasch H, Boyle E, Manov D, Sigurdson D, McNeil J, Stramska M, Michaels A, Nelson N, Siegel D, Chang G, Wu J, Knap A (1998) Initial results from the Bermuda testbed mooring program. Deep-Sea Res Pt I 45:771–794

Doney SC (1996) A synoptic atmospheric surface forcing data set and physical upper ocean model for the U.S. JGOFS Bermuda Atlantic Time-Series Study (BATS) site. J Geophys Res 101: 25615–25634

Doney SC (1999) Major challenges confronting marine biogeochemical modeling. Global Biogeochem Cy 13:705–714

Doney SC, Hecht MW (2002) Antarctic bottom water formation and deep water chlorofluorocarbon distributions in a global ocean climate model. J Phys Oceanogr 32:1642–1666

Doney SC, Sarmiento JL (eds) (1999) Synthesis and modeling project; ocean biogeochemical response to climate change. U.S. JGOFS Planning Report 22, U.S. JGOFS Planning Office, Woods Hole, MA, 105 pp

Doney SC, Glover DM, Najjar RG (1996) A new coupled, one-dimensional biological-physical model for the upper ocean: applications to the JGOFS Bermuda Atlantic Time Series (BATS) site. Deep-Sea Res Pt II 43:591–624

Doney SC, Large WG, Bryan FO (1998) Surface ocean fluxes and water-mass transformation rates in the coupled NCAR Climate System Model. J Climate 11:1422–1443

Doval M, Hansell DA (2000) Organic carbon and apparent oxygen utilization in the western South Pacific and central Indian Oceans. Mar Chem 68:249–264

Dutay J-C, Bullister JL, Doney SC, Orr JC, Najjar R, Caldeira K, Champin J-M, Drange H, Follows M, Gao Y, Gruber N, Hecht MW, Ishida A, Joos F, Lindsay K, Madec G, Maier-Reimer E, Marshall JC, Matear RJ, Monfray P, Plattner G-K, Sarmiento J, Schlitzer R, Slater R, Totterdell IJ, Weirig M-F, Yamanaka Y, Yool A (2001) Evaluation of ocean model ventilation with CFC-11: comparison of 13 global ocean models. Ocean Modelling 4: 89–120

Dutkiewicz S, Follows M, Marshall J, Gregg WW (2001) Interannual variability of phytoplankton abundances in the North Atlantic. Deep-Sea Res Pt II 48:2323–2344

England MH (1995) Using chlorofluorocarbons to assess ocean climate models. Geophys Res Lett 22:3051–3054

England MH, Maier-Reimer E (2001) Using chemical tracers to assess ocean models. Rev Geophys 39:29–70

Evans GT, Fasham MJR (ed) (1993) Towards a model of ocean biogeochemical processes. Springer-Verlag, New York

Evans GT, Garçon VC (ed) (1997) One-dimensional models of water column biogeochemistry. JGOFS Report 23/97, 85 pp., JGOFS, Bergen, Norway

Evans GT, Parslow JS (1985) A model of annual plankton cycles. Biolo Oceanogr 3:327–347

Falkowski PG, Biscaye PE, Sancetta C (1994) The lateral flux of biogenic particles from the eastern North American continental margin to the North Atlantic Ocean. Deep-Sea Res Pt II 41: 583–601

Fasham MJR (1993) Modelling the marine biota. In: Heimann M (ed) The global carbon cycle. Springer-Verlag, Heidelberg, pp 457–504

Fasham MJR (1995) Variations in the seasonal cycle of biological production in subarctic oceans: a model sensitivity analysis. Deep-Sea Res Pt I 42:1111–1149

Fasham MJR, Evans GT (1995) The use of optimisation techniques to model marine ecosystem dynamics at the JGOFS station at 47° N and 20° W. Philos T Roy Soc B 348:206–209

Fasham MJR, Ducklow HW, McKelvie SM (1990) A nitrogen-based model of plankton dynamics in the oceanic mixed layer. J Mar Res 48:591–639

Fennel K, Losch M, Schröter J, Wenzel M (2001) Testing a marine ecosystem model: sensitivity analysis and parameter optimization. J Marine Syst 28:45–63

Fennel K, Spitz YH, Letelier RM, Abbott MR, Karl DM (2002) A deterministic model for N_2-fixation at the HOT site in the subtropical North Pacific. Deep-Sea Res II 49:149–174

Francis RC, Hare SR (1994) Decadal-scale regime shifts in the large marine ecosystems of the North-east Pacific: a case for historical science. Fish Oceanogr 3:279–291

Frost BW (1987) Grazing control of phytoplankton stock in the subarctic Pacific: a model assessing the role of mesozooplankton, particularly the large calanoid copepods, *Neocalanus* spp. Mar Ecol Prog Ser 39:49–68

Fung IY, Meyn SK, Tegen I, Doney SC, John JG, Bishop JKB (2000) Iron supply and demand in the upper ocean. Global Biogeochem Cy 14:281–295

Garçon VC, Oschlies A, Doney SC, McGillicuddy D, Waniek J (2001) The role of mesoscale variability on plankton dynamics. Deep-Sea Res Pt II 48:2199–2226

Geider RJ, MacIntyre HL, Kana TM (1996) A dynamic model of photoadaptation in phytoplankton. Limnol Oceanogr 41:1–15

Geider RJ, MacIntyre HL, Kana TM (1998) A dynamic regulatory model of phytoplankton acclimation to light, nutrients, and temperature. Limnol Oceanogr 43:679–694

Gent PR, McWilliams JC (1990) Isopycnal mixing in ocean circulation models. J Phys Oceanogr 20:150–155

Gent PR, Bryan FO, Danabasoglu G, Doney SC, Holland WR, Large WG, McWilliams JC (1998) The NCAR Climate System Model global ocean component. J Climate 11:1287–1306

Giering R, Kaminski T (1998) Recipes for adjoint code construction. Acm t math software 24:437–474

Gnanadesikan A (1999) A global model of silicon cycling: sensitivity to eddy parameterization and dissolution. Global Biogeochem Cy 13:199–220

Gnanadesikan A, Toggweiler JR (1999) Constraints placed by silicon cycling on vertical exchange in general circulation models. Geophys Res Lett 26:1865–1868

Gnanadesikan A, Slater R, Gruber N, Sarmiento JL (2001) Oceanic vertical exchange and new production: a comparison between models and observations. Deep-Sea Res Pt II 49:363–401

Gregg WW (2002) Tracking the SeaWiFS record with a coupled physical/biogeochemical/radiative model of the global oceans. Deep-Sea Res Pt II 49:81–105

Griffes SM, Böning C, Bryan FO, Chassignet EP, Gerdes R, Hasumi H, Hirst A, Treguer A-M, Webb D (2000) Developments in ocean climate modelling, vol. 2. pp 123–192

Gruber N (1998) Anthropogenic CO_2 in the Atlantic Ocean. Global Biogeochem Cy 12:165–191

Gruber N, Sarmiento JL (1997) Global patterns of marine nitrogen fixation and denitrification. Global Biogeochem Cy 11: 235–266

Gruber N, Sarmiento JL, Stocker TF (1996) An improved method for detecting anthropogenic CO_2 in the oceans. Global Biogeochem Cy 10:809–837

Gruber N, Gloor M, Fan SM, Sarmiento JL (2001) Air-sea flux of oxygen estimated from bulk data: implications for the marine and atmospheric oxygen cycle. Global Biogeochem Cy 15(4): 783–803

Haidvogel DB, Beckmann A (1999) Numerical ocean circulation modeling. Imperial College Press, London, 318 pp

Haidvogel DB, Curchitser E, Iskandarani M, Hughes R, Taylor M (1997) Global modeling of the ocean and atmosphere using the spectral element method. Atmos Ocean 35:505–531

Hansell DA, Carlson CA (1998) Net community production of dissolved organic carbon. Global Biogeochem Cy 12:443–453

Harris RP (1994) Zooplankton grazing on the coccolithophore *Emiliania huxleyi* and its role in inorganic carbon flux. Mar Biol 119:431–439

Harrison DE (1996) Vertical velocity variability in the tropical Pacific: a circulation model perspective for JGOFS. Deep-Sea Res Pt II 43:687–705

Hecht MW, Wingate BA, Kassis P (2000) A better, more discriminating test problem for ocean tracer transport. Ocean Modelling 2:1–15

Heinze C, Maier-Reimer E, Schlosser P (1998) Transient tracers in a global OGCM: source functions and simulated distributions. J Geophys Res 103:15903–15922

Heinze C, Maier-Reimer E, Winguth AME, Archer D (1999) A global oceanic sediment model for long-term climate studies. Global Biogeochem Cy 13:221–250

Holfort J, Johnson KM, Wallace DWR (1998) Meridional transport of dissolved inorganic carbon in the South Atlantic Ocean. Global Biogeochem Cy 12:479–499

Holligan PM, Fernandez E, Aiken J, Balch WM, Boyd P, Burkill PH, Finch M, Groom SB, Malin O, Muller K, Purdie DA, Robinson C, Trees CC, Turner SM, van del Wal P (1993) A biogeochemical study of the coccolithophore *Emiliania huxleyi* in the North Atlantic. Global Biogeochem Cy 7:879–900

Hood RR, Bates NR, Olson DB (2001) Modeling the seasonal to interannual biogeochemical and N_2 fixation cycles at BATS. Deep-Sea Res Pt II 48:1609–1648

Hurtt GC, Armstrong RA (1996) A pelagic ecosystem model calibrated with BATS data. Deep-Sea Res Pt II 43:653–683

Ishizaka J (1990) Coupling of Coastal Zone Color Scanner data to a physical-biological model of the Southeastern U.S. continental shelf ecosystem, 3, nutrient and phytoplankton fluxes and CZCS data assimilation. J Geophys Res 95:20201–20212

Joos F, Siegenthaler U, Sarmiento JL (1991) Possible effects of iron fertilization in the Southern Ocean on atmospheric CO_2 concentration. Global Biogeochem Cy 5:135–150

Joos F, Plattner O-K, Schmittner A (1999) Global warming and marine carbon cycle feedbacks on future atmospheric CO_2. Science 284:464–467

Karl DM (1999) A sea of change: biogeochemical variability in the North Pacific subtropical gyre. Ecosystems 2:181–214

Karl DM, Letelier R, Hebel D, Tupas L, Dore J, Christian J, Winn C (1995) Ecosystem changes in the North Pacific subtropical gyre attributed to the 1991–1992 El Niño. Nature 378:230–234

Karl D, Letelier R, Tupas L, Dore J, Christian J, Hebel D (1997) The role of nitrogen fixation in biogeochemical cycling in the subtropical North Pacific Ocean. Nature 388:533–538
Kasibhatla P, Heimann M, Rayner P, Mahowald N, Prinn RG, Hartley DE (ed) (2000) Inverse methods in global biogeochemical cycles. AGU Geophysical. Monograph Series, American Geophysical Union, Washington D.C., 324 pp
Keeling RF, Piper SC, Heimann M (1996) Global and hemispheric CO_2 sinks deduced from changes in atmospheric O_2 concentration. Nature 381:218–221
Kleypas JA, Doney SC (2001) Nutrients, chlorophyll, primary production and related biogeochemical properties in the ocean mixed layer – a compilation of data collected at nine JGOFS sites. NCAR Technical Report, NCAR/TN-447+STR, 53 pp
Kleypas JA, Buddemeier RW, Archer D, Gattuso J-P, Langdon C, Opdyke BN (1999) Geochemical consequences of increased atmospheric carbon dioxide on coral reefs. Science 284:118–120
Large WG, McWilliams JC, Doney SC (1994) Oceanic vertical mixing: a review and a model with a nonlocal boundary layer parameterization. Rev Geophys 32:363–403
Large WG, Danabasoglu G, Doney SC, McWilliams JC (1997) Sensitivity to surface forcing and boundary layer mixing in a global ocean model: annual-mean climatology. J Phys Oceanogr 27:2418–2447
Laws EA, Falkowski PG, Smith WO Jr., Ducklow H, McCarthy JJ (2000) Temperature effects on export production in the open ocean. Global Biogeochem Cy 14:1231–1246
Le Quéré C, Orr JC, Monfray P, Aumont O, Madec G (2000) Interannual variability of the oceanic sink of CO_2 from 1979 though 1997. Global Biogeochem Cy 14:1247–1265
Leonard CL, McClain CR, Murtugudee R, Hofmann EE, Harding JLW (1999) An iron-based ecosystem model of the central equatorial Pacific. J Geophys Res 104:1325–1341
Letelier RM, Abbott MR (1996) An analysis of chlorophyll fluorescence for the Moderate Resolution Imaging Spectrometer (MODIS). Remote Sens Environ 58:215–223
Letelier R, Karl D (1996) Role of *Trichodesmium* spp. in the productivity of the subtropical North Pacific Ocean. Mar Ecol Prog Ser 133:263–273
Letelier R, Karl D (1998) *Trichodesmium* spp. physiology and nutrient fluxes in the North Pacific subtropical gyre. Aquat Microb Ecol 15:265–276
Levitus S, Conkright ME, Reid JL, Najjar RG, Mantilla A (1993) Distribution of nitrate, phosphate and silicate in the world oceans. Prog Oceanogr 31:245–273
Levitus S, Burgett R, Boyer T (1994) World atlas 1994. NOAA Atlas NESDIS, U.S. Dept. of Commerce, Washington D.C.
Levy M, Memery L, Madec G (1999) Combined effects of mesoscale processes and atmospheric high-frequency variability on the spring bloom in the MEDOC area. Deep-Sea Res Pt I 47:27–53
Lima I, Doney S, Bryan F, McGillicuddy D, Anderson L, Maltrud M (1999) Preliminary results from an eddy-resolving ecosystem model for the North Atlantic. EOS, Transactions AGU, 80(49), Ocean Sciences Meeting Supplement, O528
Lima ID, Olson DB, Doney SC (2002) Biological response to frontal dynamics and mesoscale variability in oligotrophic environments: a numerical modeling study. J Geophys Res (in press)
Lipschultz F, Owens NJP (1996) An assessment of nitrogen fixation as a source of nitrogen to the North Atlantic. Biogeochemistry 35:261–274
Liu K-K, Atkinson L, Chen CTA, Gao S, Hall J, Macdonald RW, Talaue McManus L, Quiñones R (2000) Exploring continental margin carbon fluxes on a global scale. EOS, Transactions of the American Geophysical Union 81:641–644
Louanchi F, Najjar RG (2000) A global monthly mean climatology of phosphate, nitrate and silicate in the upper ocean: spring-summer production and shallow remineralization. Global Biogeochem Cy 14:957–977
Mahadevan A, Archer D (2000) Modeling the impact of fronts and mesoscale circulation on the nutrient supply and biogeochemistry of the upper ocean. J Geophys Res 105:1209–1225
Maier-Reimer E (1993) Geochemical cycles in an ocean general circulation model. Preindustrial tracer distributions. Global Biogeochem Cy 7:645–677
Maier-Reimer E, Hasselmann K (1987) Transport and storage in the ocean – an inorganic ocean-circulation carbon cycle model. Clim Dynam 2:63–90
Martin JH, Knauer GA, Karl DM, Broenkow WW (1987) VERTEX: carbon cycling in the northeast Pacific. Deep-Sea Res 34:267–285
Matear RJ (1995) Parameter optimization and analysis of ecosystem models using simulated annealing: a case study at Station P. J Mar Res 53:571–607
Matear RJ, Hirst AC (1999) Climate change feedback on the future oceanic CO_2 uptake. Tellus B 51:722–733
Matear RJ, Holloway G (1995) Modeling the inorganic phosphorus cycle of the North Pacific using an adjoint data assimilation model to assess the role of dissolved organic phosphorus. Global Biogeochem Cy 9:101–119
May RM (1973) The stability and complexity of model ecosystems. Princeton University Press, Princeton New Jersey, 265 pp
McClain CR, Arrigo K, Turk D (1996) Observations and simulations of physical and biological processes at ocean weather station P, 1951–1980. J Geophys Res 101:3697–3713
McClain CR, Cleave ML, Feldman GC, Gregg WW, Hooker SB, Kuring N (1998) Science quality SeaWiFS data for global biosphere research. Sea Technol 39:10–14
McCreary JP, Kohler KH, Hood RR, Olson DB (1996) A four compartment ecosystem model of biological activity in the Arabian Sea. Prog Oceanogr 37:193–240
McGillicuddy DJ Jr., Robinson AR (1997) Eddy-induced nutrient supply and new production. Deep-Sea Res Pt I 44:1427–1450
McGillicuddy DJ Jr., Robinson AR, Siegel DA, Jannasch HW, Johnson R, Dickey TD, McNeil J, Michaels AF, Knap AH (1998) Influence of mesoscale eddies on new production in the Sargasso Sea. Nature 394:263–266
McGowan JA, Cayan DR, Dorman LM (1998) Climate-ocean variability and ecosystem response in the Northeast Pacific. Science 281:210–217
McWilliams JC (1996) Modeling the oceanic general circulation. Annu Rev Fluid Mech 28:215–248
Milliman JD (1993) Production and accumulation of calcium carbonate in the ocean: budget of a nonsteady state. Global Biogeochem Cy 7:927–957
Milliman JD, Troy PJ, Balch WM, Adams AK, Li YH, Mackenzie FT (1999) Biologically mediated dissolution of calcium carbonate above the chemical lysocline? Deep-Sea Res Pt I 46:1653–1669
Moloney CL, Field JG (1991) The size-based dynamics of plankton food webs. I. A simulation model of carbon and nitrogen flows. J Plankton Res 13:1003–1038
Moore JK, Doney SC, Kleypas JA, Glover DM, Fung IY (2002a) An intermediate complexity marine ecosystem model for the global domain. Deep-Sea Res Pt II 49:403–462
Moore JK, Doney SC, Kleypas JA, Glover DM, Fung IY (2002b) Iron cycling and nutrient limitation patterns in surface waters of the world ocean. Deep-Sea Res Pt II 49:463–507
Murnane RJ, Sarmiento JL, Le Quéré C (1999) Spatial distribution of air-sea CO_2 fluxes and the interhemispheric transport of carbon by the oceans. Global Biogeochem Cy 13:287–305
Najjar RG, Sarmiento JL, Toggweiler JR (1992) Downward transport and fate of organic matter in the ocean: simulations with a general circulation model. Global Biogeochem Cy 6:45–76
Oeschger H, Siegenthaler U, Guglemann A (1975) A box-diffusion model to study the carbon dioxide exchange in nature. Tellus 27:168–192
Orr JC, Maier-Reimer E, Mikolajewicz U, Monfray P, Sarmiento JL, Toggweiler JR, Taylor NK, Palmer J, Gruber N, Sabine CL, Le Quéré C, Key RM, Boutin J (2001) Estimates of anthropogenic carbon uptake from four three-dimensional global ocean models. Global Biogeochem Cy 15:43–60
Oschlies A (2000) Equatorial nutrient trapping in biogeochemical ocean models: the role of advection numerics. Global Biogeochem Cy 14:655–667
Oschlies A, Garçon V (1998) Eddy-induced enhancement of primary production in a model of the North Atlantic Ocean. Nature 394:266–269
Oschlies A, Garçon V (1999) An eddy-permitting coupled physical-biological model of the North Atlantic-1. Sensitivity to advection numerics and mixed layer physics. Global Biogeochem Cy 13:135–160

Polovina JJ, Mitchum GT, Evans GT (1995) Decadal and basin-scale variation in mixed layer depth and the impact on biological production in the Central and North Pacific, 1960–88. Deep-Sea Res Pt I 42:1701–1716
Pondaven P, Ruiz-Pino D, Jeandel C (2000) Interannual variability of Si and N cycles at the time-series station KERFIX between 1990 and 1995 – a 1-D modelling study. Deep-Sea Res Pt I 47:223–257
Rayner PJ, Enting IG, Francey RJ, Langenfelds R (1999) Reconstructing the recent carbon cycle from atmospheric CO_2, $d13C$ and O2/N2 observations. Tellus B 51:213–232
Reid PC, Edwards M, Hunt HG, Warner AJ (1998) Phytoplankton change in the North Atlantic. Nature 391:546
Riley GA (1946) Factors controlling phytoplankton populations on Georges Bank. J Mar Res 6:54–73
Rintoul SR, Wunsch C (1991) Mass, heat, oxygen and nutrient fluxes and budgets in the North Atlantic Ocean. Deep-Sea Res 38 (suppl.) S355–S377
Roberts M, Marshall D (1998) Do we require adiabatic dissipation schemes in eddy-resolving ocean models? J Phys Oceanogr 28:2050–2063
Robinson AR (1996) Physical processes, field estimation and an approach to interdisciplinary ocean modeling. Earth-Sci Rev 40:3–54
Robinson AR, McCarthy JJ, Rothschild BJ (2001) The sea: biological-physical interactions in the ocean. John Wiley & Sons, New York
Ryabchenko VA, Gorchakov VA, Fasham MJR (1998) Seasonal dynamics and biological productivity in the Arabian Sea euphotic zone as simulated by a three-dimensinoal ecosystem model. Global Biogeochem Cy 12:501–530
Sabine CL, Key RM, Goyet C, Johnson KM, Millero FJ, Poisson A, Sarmiento JL, Wallace DWR, Winn CD (1999) Anthropogenic CO_2 inventory in the Indian Ocean. Global Biogeochem Cy 13:179–198
Sarmiento JL, Sundquist ET (1992) Revised budget for the oceanic uptake of anthropogenic carbon dioxide. Nature 356:589–593
Sarmiento JL, Wofsy SC (1999) A U.S. Carbon Cycle Science Plan. (U.S. CCSP 1999), U.S. Global Change Research Program, Washington DC, 69 pp
Sarmiento JL, Orr JC, Siegenthaler U (1992) A perturbation simulation of CO_2 uptake in an ocean general circulation model. J Geophys Res 97:3621–3646
Sarmiento JL, Slater RD, Fasham MJR (1993) A seasonal three-dimensional ecosystem model of nitrogen cycling in the North Atlantic euphotic zone. Global Biogeochem Cy 7:417–450
Sarmiento JL, Hughes TMC, Stouffer RJ, Manabe S (1998) Simulated response of the ocean carbon cycle to anthropogenic climate warming. Nature 393:245–249
Sarmiento JL, Monfray P, Maier-Reimer E, Aumont O, Murnane RJ, Orr JC (2000) Sea-air CO_2 fluxes and carbon transport: a comparison of three ocean general circulation models. Global Biogeochem Cy 14:1267–1281
Schimel D, Enting IG, Heimann M, Wigley TML, Raynaud D, Alves D, Siegenthaler U (1995) CO_2 and the carbon cycle. In: Houghton JT, Meira Filho LG, Bruce J, Lee H, Callander BA, Haites E, Harris N, Maskell K (eds) Climate change 1994. Intergovernmental Panel on Climate Change. Cambridge University Press, pp 39–71
Schlitzer R (2000) Applying the adjoint method for global biogeochemical modeling. In: Kasibhatla P, et al. (eds) Inverse methods in global biogeochemical cycles. AGU Geophysical Monograph Series, American Geophysical Union, Washington D.C., pp 107–124
Siegenthaler U, Joos F (1992) Use of a simple model for studying oceanic tracer distributions and the global carbon cycle. Tellus B 44:186–207
Siegenthaler U, Oeschger H (1978) Predicting future atmospheric carbon dioxide levels. Science 199:388–395
Siegenthaler U, Sarmiento JL (1993) Atmospheric carbon dioxide and the ocean. Nature 365:119–125
Six KD, Maier-Reimer E (1996) Effects of plankton dynamics on seasonal carbon fluxes in an ocean general circulation model. Global Biogeochem Cy 10:559–583
Smith RD, Maltrud ME, Bryan FO, Hecht MW (2000) Numerical simulation of the North Atlantic at 1/10°. J Phys Oceanogr 30:1532–1561
Smith SV, Hollibaugh JT (1993) Coastal metabolism and the oceanic organic carbon balance. Rev Geophys 31:75–89
Spall MA, Holland WR (1991) A nested primitive equation model for oceanic applications. J Phys Oceanogr 21:205–220
Spall SA, Richards KJ (2000) A numerical model of mesoscale frontal instabilities and plankton dynamics. I. Model formulation and initial experiments. Deep-Sea Res Pt I 47:1261–1301
Spitz YH, Moisan JR, Abbott MR, Richman JG (1998) Data assimilation and a pelagic ecosystem model: parameterization using time series observations. J Marine Syst 16:51–68
Steele JH (1958) Plant production in the northern North Sea. Mar Res 7:1–36
Steele JH (1974) The structure of marine ecosystems. Harvard University Press, Cambridge, MA, 128 pp
Stephens BB, Keeling RF (2000) The influence of Antarctic sea ice on glacial/interglacial CO_2 variations. Nature 404:171–174
Stocker TF, Broecker WS, Wright DG (1994) Carbon uptake experiments with a zonally-averaged global ocean circulation model. Tellus B 46:103–122
Sunda WG, Huntsman SA (1995) Iron uptake and growth limitation in oceanic and coastal phytoplankton. Mar Chem 50:189–206
Takahashi T, Feely RA, Weiss RF, Wanninkhof RH, Chipman DW, Sutherland SC, Takahashi TT (1997) Global air-sea flux of CO_2, An estimate based on measurements of sea-air pCO_2 difference. P Natl Acad Sci USA 94:8929–8299
Takahashi T, Wanninkhof RH, Feely RA, Weiss RF, Chipman DW, Bates N, Olafson J, Sabine C, Sutherland SC (1999) Net air-sea CO_2 flux over the global oceans: an improved estimate based on the sea-air pCO_2 difference. In: Center for Global Environmental Research, National Institute for Environmental Studies (ed) Proceedings of the 2nd International Symposium on CO_2 in the Oceans. Tsukuba, Japan, pp 9–15
Tegen I, Fung I (1995) Contribution to the atmospheric mineral aerosol load from land surface modification. J Geophys Res 100:18,707–18,726
Toggweiler JR (1999) Variation of atmospheric CO_2 by ventilation of the ocean's deepest water. Paleoceanography 14:571–588
Toggweiler JR, Dixon K, Bryan K (1989a) Simulations of radiocarbon in a coarse-resolution world ocean model; 1. Steady state pre-bomb distribution. J Geophys Res 94:8217–8242
Toggweiler JR, Dixon K, Bryan K (1989b) Simulations of radiocarbon in a coarse-resolution world ocean model; 2. Distributions of bomb-produced carbon-14. J Geophys Res 94:8243–8264
US Joint Global Ocean Flux Study (US JGOFS) (1992) Report of the U.S. JGOFS Workshop on Modeling and Data Assimilation. Planning Report Number 14, U.S. JGOFS Planning Office, Woods Hole, MA, 28 pp
Venrick EL, McGowan JA, Cayan DR, Hayward TL (1987) Climate and chlorophyll a: longterm trends in the central North Pacific Ocean. Science 238:70–72
Wallace DWR (1995) Monitoring global ocean carbon inventories. Ocean Observing System Development Panel Background, Texas A&M University, College Station, TX, 54 pp
Wallace DWR (2001) Storage and transport of excess CO_2 in the oceans: the JGOFS/WOCE Global CO_2 survey. In: Siedler G, Gould J, Church J (eds) Ocean circulation and climate: observing and modeling the global ocean. Academic Press, New York
Walsh JJ (1991) Importance of continental margins in the marine biogeochemical cycling of carbon and nitrogen. Nature 350:53–55
Wanninkhof R (1992) Relationship between wind speed and gas exchange over the ocean. J Geophys Res 97:7373–7382
Wanninkhof R, Doney SC, Peng T-H, Bullister J, Lee K, Feely RA (1999) Comparison of methods to determine the anthropogenic CO_2 invasion into the Atlantic Ocean. Tellus B, 51:511–530
Watson AJ, Orr JC (2003) Carbon dioxide fluxes in the global ocean. Springer-Verlag, (this volume)
Webb DJ, deCuevas BA, Richmond CS (1998) Improved advection schemes for ocean models. J Atmos Ocean Tech 15:1171–1187
Yamanaka Y, Tajika E (1996) The role of the vertical fluxes of particulate organic matter and calcite in the oceanic carbon cycle: studies using an ocean biogeochemical general circulation model. Global Biogeochem Cy 10:361–382